frontiers in Marine Science

ORIGINAL RESEARCH
published: 13 November 2018
doi: 10.3389/fmars.2018.00394

Plankton Multiproxy Analyses in the Northern Patagonian Shelf, Argentina: Community Structure, Phycotoxins, and Characterization of Toxic *Alexandrium* Strains

Valeria A. Guinder[1,2], Urban Tillmann[3], Bernd Krock[3], Ana L. Delgado[1,2], Torben Krohn[3], John E. Garzón Cardona[1,2], Katja Metfies[3,4], Celeste López Abbate[1,2], Ricardo Silva[5] and Rubén Lara[1,2]*

[1] Instituto Argentino de Oceanografía, Consejo Nacional de Investigaciones Científicas y Técnicas, Bahía Blanca, Argentina, [2] Departamento de Biología, Bioquímica y Farmacia, Universidad Nacional del Sur, Bahía Blanca, Argentina, [3] Alfred-Wegener-Institut Helmholtz-Zentrum für Polar- und Meeresforschung, Bremerhaven, Germany, [4] Helmholtz Institute for Functional Marine Biodiversity, Oldenburg, Germany, [5] Instituto Nacional de Investigación y Desarrollo Pesquero, Mar del Plata, Argentina

OPEN ACCESS

Edited by:
Marius Nils Müller, Universidade Federal de Pernambuco, Brazil

Reviewed by:
Jelena Godrijan, Bigelow Laboratory for Ocean Sciences, United States
Carnicer Olga, Pontificia Universidad Católica del Ecuador, Ecuador

***Correspondence:**
Valeria A. Guinder
vguinder@criba.edu.ar

Specialty section:
This article was submitted to Marine Ecosystem Ecology, a section of the journal Frontiers in Marine Science

Received: *25 May 2018*
Accepted: *09 October 2018*
Published: *13 November 2018*

Citation:
Guinder VA, Tillmann U, Krock B, Delgado AL, Krohn T, Garzón Cardona JE, Metfies K, López Abbate C, Silva R and Lara R (2018) Plankton Multiproxy Analyses in the Northern Patagonian Shelf, Argentina: Community Structure, Phycotoxins, and Characterization of Toxic Alexandrium Strains. Front. Mar. Sci. 5:394. doi: 10.3389/fmars.2018.00394

The extensive Argentine continental shelf supports high plankton productivity and fish catches. In particular, El Rincón coastal area and the adjacent shelf fronts (38.5–42°S, 58.5–62°W) comprise diverse habitats and hold species of economic and ecological value. So far, studies of the microbial community present at the base of the food web remain scarce. Here, we describe the late winter plankton (5–200 μm) structure in terms of abundance, biomass, species composition, functional groups, and phycotoxin profiles in surface waters of El Rincón in September 2015. Diatoms are the most abundant and the largest contributors to carbon biomass at most stations. They dominated the coastal and inner-shelf (depths <50 m), while dinoflagellates and small flagellates (<15 μm) dominated offshore at the middle-shelf waters (depth ∼100 m). In addition, large (>20 μm) heterotrophic protists such as various ciliates and dinoflagellates species were more abundant offshore. Scanning of phycotoxins disclosed that paralytic shellfish poisoning (PSP) toxins were dominated by gonyautoxins-1/4 (GTX1/4), whereas lipophilic toxins were detected in low abundance, for example, domoic acid (DA). However, a bloom of *Pseudo-nitzschia* spp. (up to 3.6×10^5 cells L^{-1}) was detected at inner-shelf stations. Pectenotoxin-2 (PTX-2) and 13-desmethyl spirolide C (SPX-1) were the most abundant in the field. The PTX-2 co-occurred with *Dinophysis* spp., mainly *D. tripos*, while SPX-1 dominated at middle-shelf stations, where cells of *Alexandrium catenella* (1 strain) and *A. ostenfeldii* (3 strains) were isolated. The quantitative PSP profiles of the *Alexandrium* strains differed significantly from the *in situ* profiles. Moreover, the three *A. ostenfeldii* strains produced PSP and additionally, five novel spirolides. Phylogenetic analyses of these newly isolated strains

from the South Atlantic revealed a new ribotype group, suggesting a biogeographical distinction in the population. The plankton survey presented here contributes baseline knowledge to evaluate potential ecosystem changes and track the global distribution of toxigenic species.

Keywords: protists' plankton, functional groups, shelf front, phycotoxins, *Alexandrium ostenfeldii*, novel spirolides, Patagonian Shelf, SW Atlantic

INTRODUCTION

Shelf seas play a major role in ocean carbon cycling and budget, as a large part of the global marine primary production takes place in the coastal areas, and about half of this organic carbon is exported to the deep ocean (Liu et al., 2010). The Patagonian Shelf Large Marine Ecosystem (PLME) (Heileman, 2009) is one of the widest in the world, one of the most productive (Lutz et al., 2010), and hydrographically complex in the Southern Hemisphere (Palma et al., 2008; Matano et al., 2010; Paniagua et al., 2018). The extensive shelf breakfront and other shelf fronts support high phytoplankton productivity and fisheries incomes (Acha et al., 2004; Carreto et al., 2016; Carranza et al., 2017; Díaz et al., 2018). Moreover, recent studies on satellite images showed that chlorophyll *a* (chl-*a*) has notably risen over the last two decades (Marrari et al., 2017), which highlights the role of this large ecosystem in the global carbon uptake and in the regional sustainability of marine resources and stakeholder communities (Bianchi et al., 2009; Marrari et al., 2013). Hence, the identification of the phytoplankton responsible for high productivity, concerning beneficial and harmful blooms, becomes essential to track changes in the food web and manage potential risk for the biota and human health.

In particular, the area of the Argentine shelf called El Rincón extends from 38.5°S to approximately 42°S (**Figure 1**) and is especially wide at some areas, that is, ∼300 km (Lucas et al., 2005). El Rincón ecosystem, with its middle-shelf front (located at ∼100 m isobaths, Romero et al., 2006), embraces large habitat heterogeneity (Lucas et al., 2005; Palma et al., 2008) characterized by high zooplankton and fish biodiversity (*e.g.,* Marrari et al., 2004; López Cazorla et al., 2014; Acha et al., 2018). For instance, its frontal areas are the main spring reproductive habitats of the northern stock of Argentine anchovy (*Engraulis anchoita*) (Marrari et al., 2013; Díaz et al., 2018) and other valuable species (*e.g.,* Hoffmeyer et al., 2009; Marrari et al., 2013; Acha et al., 2018). So far, there has been only one study on the planktonic microorganisms of El Rincón (Negri et al., 2013) and few of the adjacent areas (Silva et al., 2009; Segura et al., 2013), and they are mainly focused on the smallest cell sized fractions. Along the Argentine shelf fronts and shelf- breakfront, spatial heterogeneity of the phytoplankton composition has been related to contrasting nutritional properties of water masses (Subantarctic Shelf waters and Malvinas Current waters) and the latitudinal and cross-shelf progression in the timing of the spring bloom (García et al., 2008; Ferreira et al., 2013; Olguín et al., 2015; Carreto et al., 2016). Analyses of satellite images of the ocean color (Romero et al., 2006; Dogliotti et al., 2009; Delgado et al., 2015; Marrari et al., 2017) in combination with field *in situ* chlorophyll estimation (Lutz et al., 2010) have detected phytoplankton blooms in spring and summer (maxima between October and February). Harmful algal blooms (HABs) have been documented in the Argentine shelf for the last 30 years, mainly associated with paralytic shellfish toxins (PSTs) produced by dinoflagellates of the genus *Alexandrium* (Carreto et al., 1981, 2001; Montoya et al., 2010; Almandoz et al., 2014; Fabro et al., 2017). Severe detrimental consequences in the food web, ecosystem services, and human health have been attributed to these toxic events (Benavides et al., 1995; Montoya et al., 1996; Gayoso and Fulco, 2006). Other toxigenic species and associated toxins were registered in the shelf and frontal areas, for instance, dinoflagellates of the genus *Dinophysis* (Sar et al., 2012; Fabro et al., 2016) and diatoms of the genus *Pseudo-nitzschia* (Negri et al., 2004; Almandoz et al., 2007, 2017). Blooms composed of various species of *Azadinium* spp. and *Amphidoma* spp., two genera known for the production of azaspiracids (AZAs) (Tillmann, 2018a), have been described from the Argentine shelf (Akselman and Negri, 2012; Tillmann et al., 2018; Tillmann and Akselman, 2016; Tillmann, 2018b), but the production potential of AZAs by the local species/populations is yet known only for *Azadinium poporum* (Tillmann et al., 2016). The analyses of phytoplankton composition and toxin production may lead to the understanding of carbon fluxes through the pelagic food web and to the benthos, where large beds of the scallop *Zygochlamys patagonica* are located (Bogazzi et al., 2005; Franco et al., 2017). The aim of this work is to characterize the plankton community in El Rincón including the detection of phycotoxins and toxic species. Particular interest is focused on the species of the dinoflagellate, *Alexandrium*, isolated at the middle-shelf, as this genus is of major concern due to its tendency to form HABs and its global biogeographical distribution (Anderson et al., 2012).

MATERIALS AND METHODS

Field Sampling

An oceanographic expedition on board the vessel *Bernardo Houssay* was carried out from the 5th to the 9th of September 2015 in the northern Patagonian shelf in the Argentine Sea. Twenty-four study stations were sampled in El Rincón (38°50′–41°S, 60–62°W) (**Figure 1**) (coastal, inner-shelf), which is an area encompassed between the coast and the isobath of 50 m depth and between the Bahía Blanca Estuary in the north and the Negro River Estuary in the south. In addition, two offshore stations, 33 and 34, located at the middle-shelf at 100 m depth (**Figure 1**), were sampled in the same expedition.

At each study station, surface water temperature (±0.2°C) and salinity (±0.06) were measured *in situ* by triplicate readings

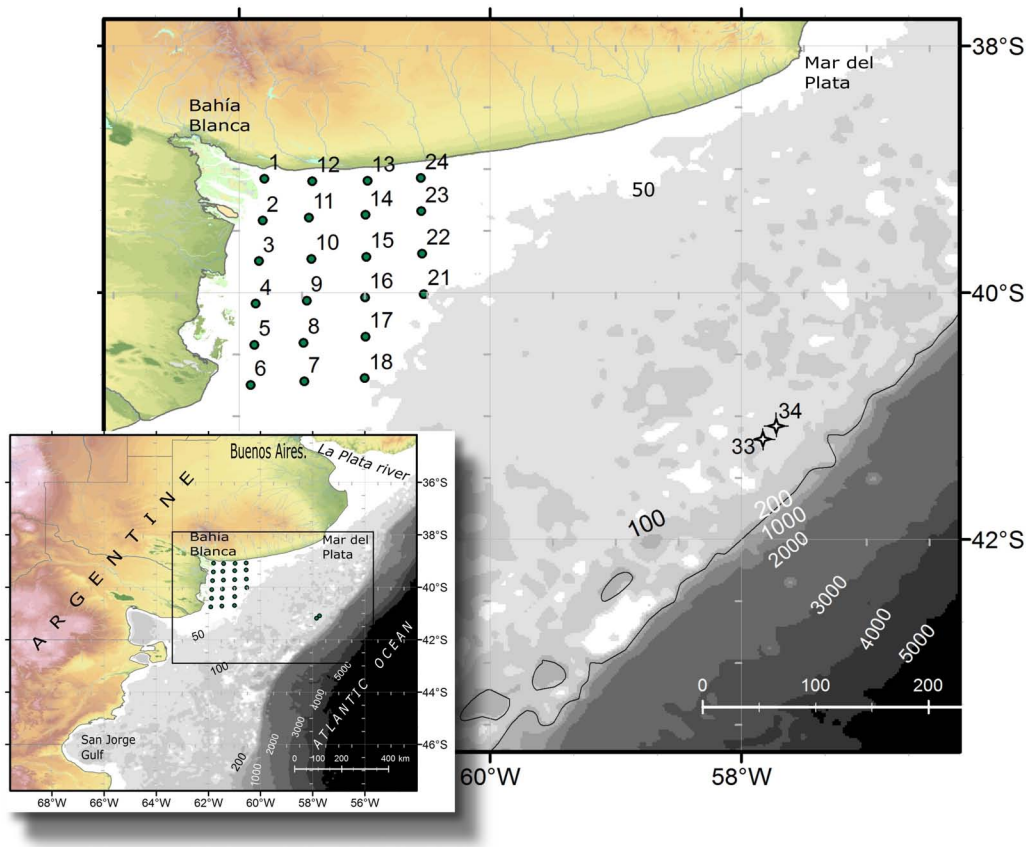

FIGURE 1 | Study area and location of the sampling stations during the oceanographic expedition in September 2015 aboard the research vessel *B. Houssay*.

with a multiparameter probe (Horiba U-10, Japan). Using Niskin bottles, surface water samples were collected for quantification of plankton and estimations of chl-*a*. For the former, 250 mL were fixed with Lugol's solution (1% final concentration) and kept in the dark until analysis under the microscope, while for chl-*a*, a volume of 200–250 mL was filtrated onboard through filter GF/C and kept at −20°C. Then, pigments were extracted using acetone:water (9:1) and the quantification was performed with a spectrofluorophotometer RF-5301PC Shimadzu calibrated with a standard of *Anacystis nidulans,* according to Holm-Hansen et al. (1965). In addition, using plankton net with a mesh of 35 μm, water samples were collected and fixed with formaldehyde (2% final concentration) for the identification of plankton species.

Chlorophyll *a* and Sea Surface Temperature (SST) From Satellite Observations

Satellite data was obtained from the Moderate Resolution Imaging Spectroradiometer (MODIS) on board the satellite Aqua. Daily level 1A data at 1 km spatial resolution, from 15th August to 30th September 2015, were downloaded from the Ocean Color website[1]. The files were processed into L2 and L3 product files using SeaDAS software, version 7.4 (Fu et al., 1998). The standard NASA atmospheric correction algorithm was applied, which provided the best performance in the optically complex waters of the studied area (Delgado et al., 2018) and other coastal waters (*i.e.*, Jamet et al., 2011; Goyens et al., 2013). The Chl-*a* and sea surface temperature (SST) products were derived from the OCx (Hu et al., 2012) and the non-linear sea surface temperature (NLSST) (Brown and Minnet, 1999) algorithms, respectively. Then, L3 products of 15 days (15th–31st August, 1st–15th September, and 16th–30th September) were obtained from the L2 (1 km) products using arithmetic averaging in Mercator projection (Campbell et al., 1995; Antoine, 2004).

Plankton Analysis

For quantitative estimations, plankton cells >5 μm were enumerated with a Wild M20 inverted microscope according to the procedures described by Hasle (1978). Depending on the seston content, subsamples of 10 mL (coastal stations) or 50 mL of seawater were collected with Niskin bottles, preserved with Lugol's solution, and were settled in Utermöhl composite sedimentation chambers during 24 h. The entire chamber was analyzed under a magnification of 400×. Plankton abundance was then expressed in cells L^{-1}. Samples of plankton at stations 4, 15, and 24 were not available. Unidentified organisms other than

[1]https://oceancolor.gsfc.nasa.gov

diatoms, dinoflagellates, and coccolithophores were classified as "flagellates" (regardless of flagella visible or not) and according to their size. Concerning dinoflagellates, species of the genera *Protoperidinium, Gyrodinium,* and some cf. *Gymnodinium*, ciliates, and the thecamoeba, *Paulinella ovalis,* were counted as heterotrophic protists. Plankton identification was performed in net haul samples under a Zeiss Standard R microscope and a Nikon Eclipse microscope, using phase contrast and differential interference contrast (DIC) and a magnification of 1000×. Local literature was consulted for the identification of plankton taxonomy from the Argentine Sea (references in the text) and general literature for identification of phytoplankton (Tomas, 1997; Hoppenrath and Debres, 2009). No cells of *Dinophysis* spp. were detected in surface bottle samples, while the associated toxin pectenotoxin-2 (PTX-2) was detected in net samples; the latter was analyzed to quantify their abundances and expressed in cells per net tow (cells NT^{-1}).

Cell dimensions were measured throughout the counting procedure using an ocular micrometer. Cell volumes of plankton (in μm^3) were calculated assigning simple geometric shapes to species according to Hillebrand et al. (1999) and transformed into carbon content (pg C $cell^{-1}$) using two different carbon-to-volume ratios, one for diatoms and one for all the other algae groups (Menden-Deuer and Lessard, 2000).

Sampling of Phycotoxins

Samples of plankton were collected by horizontal net tow hauls with a 35-μm mesh of 40-cm diameter. Net haul concentrates were adjusted to a defined volume of 2–5 L (depending on the net tow volume) using 0.2 μm filtered seawater. An aliquot of 100 mL was fixed with acidic Lugol's iodine solution (1% final concentration) for identification of the species. From the remaining volume, plankton was collected on a 20-μm mesh and transferred to a 50-mL centrifugation tube, which was adjusted to a final volume of 45 mL with filtered seawater. This sample was split into three aliquots, and each aliquot was centrifuged at a maximum speed of 3,500 × *g* in a 15-mL centrifugation tube (model 2036, Rolco, Buenos Aires, Argentina). The supernatants were discharged, pellets were resuspended in approximately 1 mL filtered sea water, transferred to a 2-mL cryovial, and centrifuged again (10 min, 3220 × *g*, model 5415 D, Eppendorf, Hamburg, Germany). Finally, supernatants were removed and cell pellets frozen at −20°C. A quantitative comparison of toxin abundances in the net tows of this expedition was not possible due to technical difficulty. Net tows could not be performed in a standardized way. No net sample could be taken at station 34.

Isolation of *Alexandrium* spp.

At stations 33 and 34, 2 L of seawater from 10 m depth were filled into different 500 mL PE flasks and kept at 4°C until inspection. Single cells of *Alexandrium* spp. were isolated from these samples by micropipette after analyzing under a stereomicroscope (SZH-ILLD, Olympus, Hamburg, Germany). Cells were transferred into individual wells of 96-well tissue culture plates (TPP, Trasadingen, Switzerland) containing 300 μL of Keller medium (Keller et al., 1987), prepared from 0.2 μm sterile-filtered natural Antarctic seawater at 1/10th of the original concentration. Isolated cells were then incubated at 15°C at a photon flux density of 50 μmol photons m^{-2} s^{-1} on a 16:8 light:dark (L:D) photocycle. After 3–4 weeks, four unialgal and clonal isolates (provisionally named H-3-D10, H-1-G8, H-3-D4, and H-2-A4), all originating from station 33, were transferred to polystyrene cell culture flasks, each containing 50 mL of ½ strength K medium and were maintained, thereafter, under the same conditions as described. Observation of live or fixed cells was carried out with a stereomicroscope (SZH-ILLD, Olympus) and with an inverted microscope (Axiovert 200 M, Zeiss, Munich, Germany) equipped with epifluorescence and DIC optics. Light microscopic examination of the thecal plate tabulation was performed on neutral lugol-fixed cells (1% final concentration) stained with calcofluor white (Fritz and Triemer, 1985). Photographs were taken with a digital camera (Axiocam MRc5, Zeiss).

For harvest of cellular DNA and analyzing of toxin, cultures of all strains were grown in 250 mL cell culture flasks at 15°C under a photon flux density of 50 μmol m^{-2} s^{-1} on a 16:8 h light:dark photocycle. In each harvest, cell density was determined by settling Lugol-fixed samples and counting cells >800 under an inverted microscope. For DNA extraction, 50 mL of culture were centrifuged as described later. For toxin analysis, 200 mL of cultures were harvested as 4 × 50 mL in 50-mL centrifugation tubes by centrifugation (Eppendorf 5810R, Hamburg, Germany) at 3,220 *g* for 10 min. Supernatant was discarded and all four pellets from one isolate were combined in a microcentrifuge tube and again centrifuged (Eppendorf 5415, 16,000 × *g*, 5 min) and stored frozen (−20°C) until use.

DNA Extraction and Phylogeny

For phylogenetic analyses of *Alexandrium* strains, genomic DNA was isolated using the E.Z.N.A Plant DNA Kit (Omega Bio-tek Inc., Norcross, GA, United States). The original isolation protocol was modified by insertion of an additional washing step using "SPW wash buffer." A NanoDrop ND-1000 system (PEQLAB, Erlangen, Germany) was used to determine the concentration and the purity of the genomic DNA. Phylogenetic inferences were based on analyses of the D1/D2 region of the 28S large subunit (LSU). The fragment of the LSU was amplified with the universal primer set D1R-F (5′ACCCGCTGAATTTAAGCATA3′) and D2C-R (5′CCTTGGTCCGTGTTTCAAGA3′) (John et al., 2014). The polymerase chain reaction (PCR) cocktail of a final volume of 50 μL contained ∼ 20 ng genomic DNA as template, 1× amplification buffer (5 Prime, Hamburg, Germany), 0.1 mM dNTPs (5 Prime), 0.1 μM of each primer, and 0.05 U of HotMaster Taq DNA Polymerase (5 Prime). The amplification protocol was performed for 2 min at 94°C, 30 s at 94°C, 30 s at 55°C, and 2 min at 68°C for 35 cycles and an extension for 10 min at 68°C. The correct size of the amplified PCR fragment was determined on a 1.5% agarose gel. The PCR product was purified with the NucleoSpin Gel and PCR cleanup kit (Macherey und Nagel, Düren, Germany) according the manufacturer's protocol and subjected to sequencing via standard BigDye Terminator v3.1 cycle sequencing chemistry (Applied Biosystems, Darmstadt, Germany). The resulting sequences were assembled using the DNASTAR software package (Lasergene,

United States). The LSU sequences obtained in this study were deposited in the GenBank database and the accession numbers are: BankIt2158787 H-2-A4 MK059419, BankIt2158787 H-1-G8 and MK059420 BankIt2158787 H-3-D4 MK059421. The sequences of the studied strains of *Alexandrium ostenfeldii* (H-2-A4, H-1-G8, and H-3-D4) were compared with 36 of other representative *A. ostenfeldii*/*A. peruvianum* strains obtained from GenBank. The LSU sequences of *Alexandrium insuetum* and *Alexandrium minutum* were used as outgroups to root the tree. The sequence of the *Alexandrium catenella* strain (H-3-D10) was compared with the LSU sequence assemblage, which is used to formally revise the *Alexandrium tamarense* species with complex taxonomy (John et al., 2014).

The MEGA7 (Kumar et al., 2016) was used for sequence alignment. The LSU sequences were aligned using ClustalW. The final alignment for the LSU phylogeny consisted of 572 positions for both *Alexandrium ostenfeldii* and *Alexandrium catenella*. The phylogenetic model was selected using the MEGA7 software package. The phylogenetic trees were represented using the maximum likelihood (ML) results, with bootstrap values from the ML method (n = 1000 replicates).

TABLE 1 | Mass spectrometric (ms) parameters used for analysis.

	PREC	EMS	CID	SRM
Curtain gas [au]	20	20	20	20
Collision gas [au]	High	Low	High	Medium
ESI voltage [V]	5500	5500	5500	5500
Temperature [°C]	650	650	650	650
Spray gas [au]	40	40	40	40
Auxiliary gas [au]	70	70	70	70
Interface heater	ON	ON	ON	ON
Declustering potential [V]	121	121	121	121
Collision energy spread [V]	–	0	0	–
Entrance potential [V]	10	5	–	10
Collision energy [V]	57	–	57	57
Collision exit potential [V]	22	–	–	22

PREC, precursor ion scan; EMS, enhanced mass scan; CID, collision-induced dissociation; SRM, selected ion monitoring; au, arbitrary units.

Analysis of Toxin of Field Samples

Cell pellets from the plankton net tows were resuspended in 500 μL of 0.03 M acetic acid for PST analysis and in 500 μL methanol for the determination of lipophilic toxins and subsequently homogenized with 0.9 g of lysing matrix D by reciprocal shaking at maximum speed (6.5 m s^{-1}) for 45 s in a Bio101 FastPrep instrument (Thermo Savant, Illkirch, France). After homogenization, samples were centrifuged at 16,100 × g at 4°C for 15 min. The supernatants were transferred to spin filters (0.45 μm pore size, Millipore Ultrafree, Eschborn, Germany) and centrifuged for 30 s at 800 × g, followed by transfer to autosampler vials.

Analysis of multiple lipophilic toxins was performed by liquid chromatography coupled with tandem mass spectrometry (LC-MS/MS) (AWI, Bremerhaven, Germany), as described by Krock et al. (2008). Contents of the toxin are expressed as nanograms per net tow (ng NT^{-1}). Paralytic shellfish poisoning (PSP) toxins were analyzed by ion-pair chromatography coupled with postcolumn derivatization and fluorescence detection (PCOX method) as described in detail by Van de Waal et al. (2015).

Analysis of Toxin of *Alexandrium* Cultures

In addition to a general screening of the selected variants of different groups of lipophilic phycotoxins, *A. ostenfeldii* strains were specifically analyzed for the presence of a wide variety of spiroimines. For spirolides, precursor ion experiments (PRECs) for the characteristic spirolide fragments m/z of 150, 164, and 180 were performed for the search of spirolide variants. For gymnodimines (including unknown variants), enhanced mass scans (EMSs) in the mass range of m/z 480–550 were performed. Collision-induced dissociation (CID) spectra of all positive m/z values detected with the before-mentioned experiments were recorded in the mass range of m/z 150–750. Applied mass spectrometric (MS) parameters are detailed in **Table 1**. All positively confirmed spiroimines were quantified in the selected reaction monitoring (SRM) mode using the mass transition listed in **Table 2** and calibrated against an external SPX-1 standard curve with four concentrations in the range from 1 to 1,000 pg μl^{-1} (Certified Reference Materials Program, NRC IMB, Halifax, NS, Canada). Results are expressed as SPX-1 equivalents.

Data Analyses of the Structure of Plankton

The distribution of the functional groups of plankton and potential toxic species in the studied area was analyzed by colored maps using the software Ocean Data View, version ODV 4.7.10. Non-parametric Spearman's correlation analyses were employed to determine correlations between chlorophyll concentration, phytoplankton abundance, and biomass. Cluster analysis was applied to the stations to assess the spatial structure of plankton, where the abundance (in cells L^{-1}) was log-transformed to normalize data. A matrix of similarities between each pair of sampling station was calculated using the Bray-Curtis similarity index. Then, the groups that were revealed by SIMPROF test in the cluster analysis were pointed out to in the map. The organisms with higher contribution to differences among groups were identified by means of SIMPER (similarity percentages) test. Statistical analysis was performed using the software PRIMER (Clarke and Gorley, 2006).

RESULTS

SST, Salinity, and Chlorophyll *a*

Surface temperature was measured *in situ* in the coastal, inner-shelf (21 stations with depth <50 m), and it varied between 10.0 and 11.3°C with a mean value of 10.4 ± 1.0°C, whereas lowest values of 7.5 and 7.2°C were detected at middle-shelf stations viz. 33 and 34. Salinity values ranged between 32.6 and

TABLE 2 | Mass transitions (Q1 and Q3 masses) used for the screening and quantification of spiroimines and corresponding spiroimines.

Q1 mass (m/z)	Q3 mass (m/z)	Spiroimine	Q1 mass (m/z)	Q3 mass (m/z)	Spiroimine
508	490	GYM A	666	180	Unspecified
510	492	desMe-GYM D	674	164	Unspecified
522	504	12-Methyl-GYM A	678	150	Unspecified
524	506	GYM A/B/D	678	164	13,19-didesMethyl-spirolide C/13/19,31-didesMethyl-spirolide C
526	508	oxo-desMe-GYM D	686	164	Unspecified
534	150	Unspecified	692	150	Spirolide A
536	150	Unspecified	692	164	13-desMethyl-spirolide C spirolide G
540	164	Unspecified	692	178	27-oxo-13,19-didesMethyl-spirolide C
540	522	Unspecified	694	150	Spirolide B
542	524	Unspecified	694	164	13-desMethyl-spirolide D Pinnatoxin G
548	530	Unspecified	694	180	27-hydroxy-13,19-didesMethyl-spirolide C
552	150	Unspecified	696	164	Unspecified
564	546	Unspecified	698	164	Unspecified
582	564	Unspecified	706	164	Spirolide C 20-Methyl-spirolide G
592	164	Spirolide M	708	164	Spirolide D
618	164	Compound 1	708	180	27-hydroxy-13-desMethyl-spirolide C
628	150	Unspecified	710	150	Unspecified
640	164	Unspecified	710	164	Compound 2
644	164	Unspecified	718	164	Compound 3
650	164	Spirolide H	720	164	Unspecified
652	164	Spirolide I	722	164	Unspecified
658	150	Unspecified	722	180	Unspecified
658	164	Unspecified	766	164	Pinnatoxin F
666	164	Unspecified	784	164	Pinnatoxin E

35 with a mean of 34.1 ± 0.7, displaying lower values at coastal stations 2–10 and at stations 33 and 34. The satellite estimations of the three 15-days means of SST (**Figures 2A–C**) and chl-*a* distribution (**Figures 2D–F**) showed that SST increased from August to September (**Figures 2A–C**) in the coastal and the inner-shelf (8–13°C), while they remained rather constant and cooler (∼5–6°C) in the middle-shelf. Conversely, chl-*a* displayed larger variability in the middle-shelf (**Figures 2D–F**), with higher values during the first half of September (**Figure 2E**) when the expedition was performed. The *in situ* chl-*a* ranged from 0.2 to 1.9 $\mu g\ L^{-1}$ (**Figure 3A**), with a mean of 0.8 ± 0.48 $\mu g\ L^{-1}$.

Total Abundance, Biomass, and Composition of Plankton

The abundance of photosynthetic protists ("phytoplankton") >5 μm was found between 0.21 × 10^5 cells L^{-1} and 6.47 × 10^5 cells L^{-1} (**Figure 3A**), with values more than twofold the mean of 1.5 × 10^5 cells L^{-1} occurring only at a few stations: 1, 5, 22, 23, and 34 (**Figure 3A**). Biomass of phytoplankton varied between 3.8 and 103.1 $\mu g\ C\ L^{-1}$ (**Figure 3A**) and both the total abundance and biomass of plankton displayed weak linear correlation with chl-*a* concentration (R^2 ∼0.56, n = 21). Abundance of heterotrophic protists was found between 3.5 × 10^3 cells L^{-1} and 1.8 × 10^5 cells L^{-1} and showed larger values in the middle-shelf (**Figure 3B**), mainly caused by high abundance of dinoflagellates. A frequent heterotrophic flagellate identified in the study area was *Leucocryptos* sp. (length 7–13 μm), and the thecamoeba *Paulinella ovalis* was seen frequently at the coastal stations (1–14). Naked ciliates ∼20 μm were observed commonly offshore (max. 5.95 × 10^4 cells L^{-1} at station 34), while tintinnids were dominant at the coastal stations close to the Bahía Blanca Estuary (station 1, 2, and 12), with low abundance (max. 7 × 10^3 cells L^{-1} at station 2).

Diatoms were the dominant group in the study area, achieving more than 50% of the abundance and the biomass of total phytoplankton at most of the stations (**Figures 4**, **5**), with the exception of stations 7, 8, 14, 16, 18, and 34, where the groups flagellates and/or dinoflagellates were more abundant (**Figures 4**, **5**). Diatoms showed the highest concentrations at the coastal stations (**Figure 5**), mainly represented by *Cymatosira belgica, Asterionellopsis glacialis*, *Paralia sulcata,* and *Thalassionema nitzschioides*, each species with abundances between 1.3 × 10^5 cells L^{-1} and 2.3 × 10^5 cells L^{-1} (list of species in **Supplementary Table 1**). In particular, diatoms displayed high concentrations at stations 22 and 23 (**Figure 5**) due to a bloom of *Pseudo-nitzschia* spp. with abundances up to 3.6 × 10^5 cells L^{-1} (**Figure 6**). At station 33, the diatom *Eucampia cornuta* reached a high concentration (8.0 × 10^4 cells L^{-1}). Two silicoflagellates were common in the study area, *Dictyocha speculum* and *D. fibula*, with maximal abundance at station 34 (3.7 × 10^4 cells L^{-1}). Dinoflagellates were more abundant at stations 33 and 34, followed by stations 21 and 22 (**Figure 5**), with dominance of heterotrophic dinoflagellates such as cf. *Gymnodinium*, *Protoperidinium* spp., *Torodinium robustum, Gyrodinium spirale,* and *Amphidinium* spp. Among the photosynthetic dinoflagellates, the most frequent were *Prorocentrum* spp., *Oxytoxum* sp., *Tripos* spp., and *Scrippsiella* sp. Small photosynthetic thecate dinoflagellates (length ∼10–18 μm) were present as well such as *Heterocapsa* sp. and species of the family Amphidomataceae (e.g., *Amphidoma parvula*, Tillmann et al., 2018), which will be further presented in detail in a companion paper (Tillmann et al. in prep). Cells of the genus *Alexandrium* were found at relatively low abundances, up to 1.0 × 10^3 cells L^{-1}, and *Dinophysis* was not detected in bottle samples, but recorded in net samples with up to 3.6 × 10^3

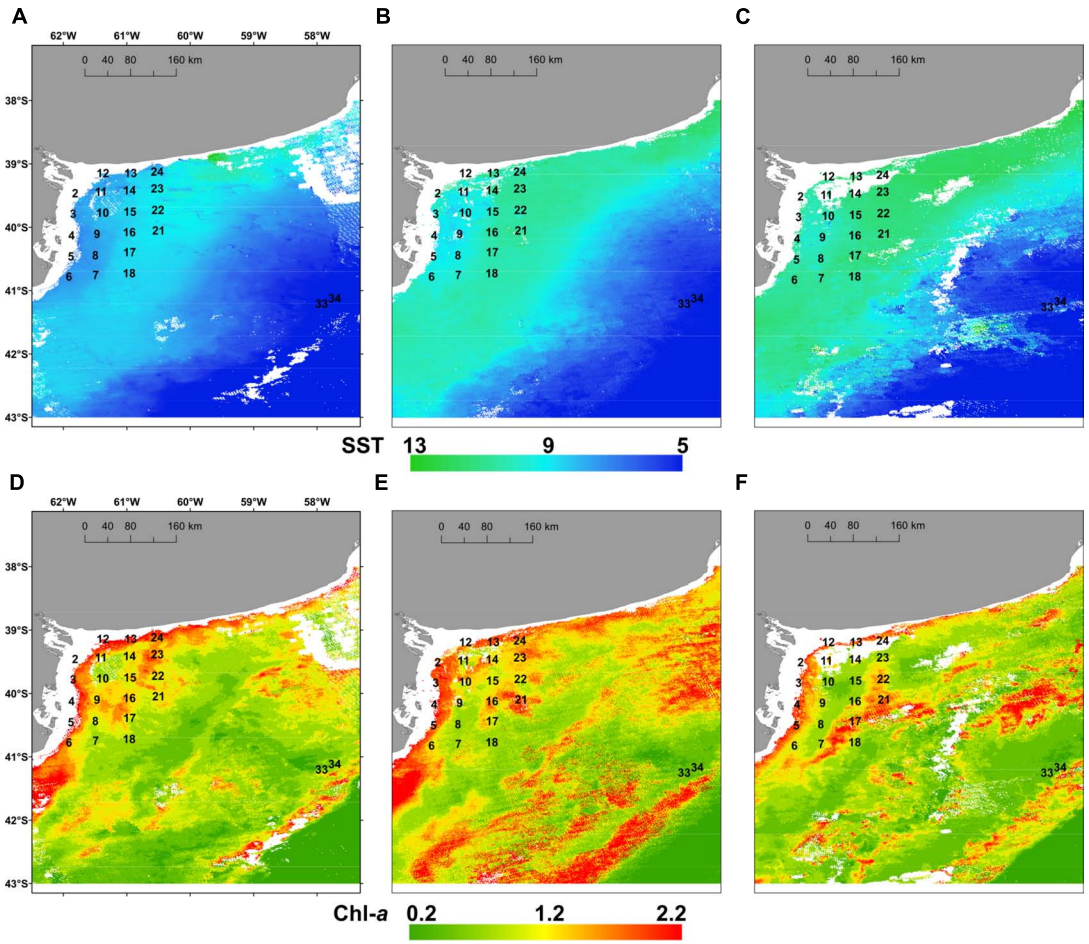

FIGURE 2 | Mean sea surface temperature, SST (°C) (upper panels) and mean surface chlorophyll *a*, chl-*a* (μg L^{-1}) (lower panels) registered by satellite images in the study area for the periods: **(A,D)** 15th–31st August 2015; **(B,E)** 1st–15th September 2015 and **(C,F)** 16th–30th September 2015.

cells NT^{-1} (**Figure 6**). The group of coccolithophores was mainly represented by *Gephyrocapsa oceanica* (5–10 μm), with the highest concentration at station 12 (3.1×10^4 cells L^{-1}), followed by *Emiliania huxleyi* (3–7 μm) at the offshore stations (up to 7.4×10^3 cells L^{-1} at station 33). The Xanthophyceae *Ophiocytium* sp. at the coastal stations and the mixotrophic ciliate *Mesodinium rubrum* at station 34 notably contributed to the total carbon biomass (**Figure 4**) due to their large cell size. The analysis of the plankton structure in the study area displayed spatial differentiation across the coastal and inner-shelf to middle-shelf stations (**Figure 7**), with decreasing ratios of diatoms to dinoflagellates and a rising trend of heterotrophic protists (**Figures 3**, **5**).

Description of the *Alexandrium* spp. Strains

Based on thecal plate pattern determined under the fluorescence microscope, three of the strains (H-1-G8, H-3-D4, and H-2-A4) were identified as *A. ostenfeldii,* whereas the fourth strain (H-3-D10) was of the *tamarense/catenella* morphotype. Cells of the strain H-3-D10, during exponential growth in culture, mainly occurred in short two-cell chains, but occasionally were present in four-cell chains. For all strains of *A. ostenfeldii*, pairs of cells probably representing late stages of cell division were regularly observed.

Cells of H-3-D10 had a typical *Alexandrium* outline with a conical epitheca and a more trapezoidal hypotheca (**Figures 8A–I**). Cells sizes ranged from 26.4 to 42.9 μm in length (mean 35.4 ± 3.1, n = 30) and from 30.0 to 39.7 μm in width (mean 35.0 ± 2.2, n = 30). The number, size, and shape of thecal plates (**Figures 8C–G**) conformed to the species description of *Alexandrium catenella*. The first apical plate consistently had a small ventral pore (**Figure 8D**). A large connecting pore was occasionally seen on both the pore plate (**Figure 8E**) and the posterior sulcal plate (**Figure 8H**).

Cells of *A. ostenfeldii* were variable in size and shape (**Figures 8J–R**), with most cells being round to slightly ellipsoid (**Figures 8J,K**). Cell length ranged from 27.7 to 43.1 μm (mean 35.4 ± 4.5, n = 30) and width from 27.4 to 42.6 μm (mean 34.7 ± 4.2, n = 30). The plate pattern (**Figures 8L–P**) and the typical shape of the first apical plate and the large ventral pore

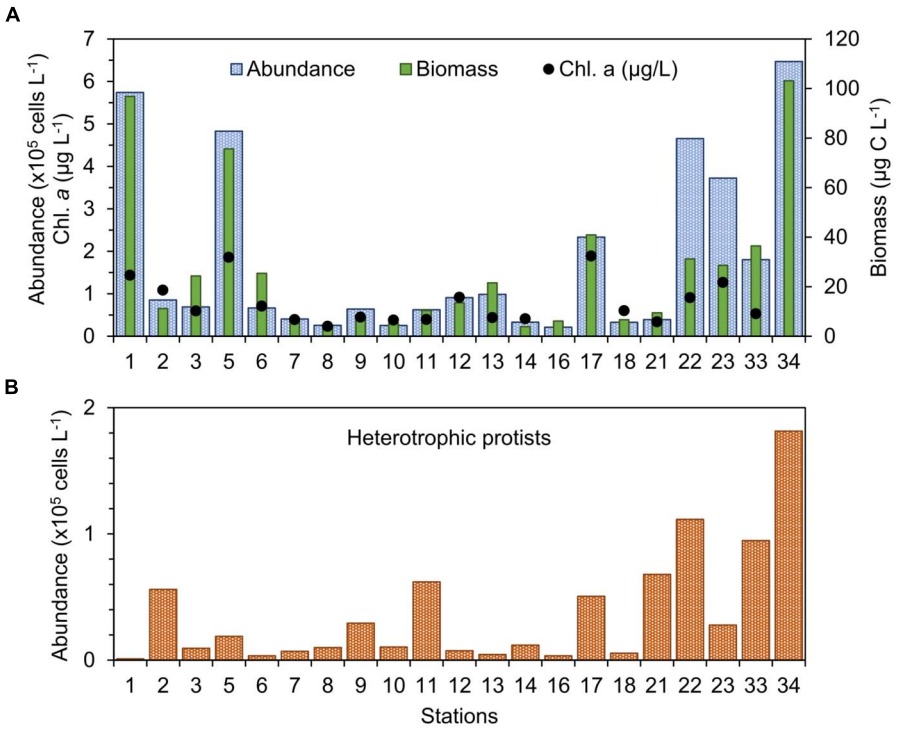

FIGURE 3 | (A) Abundance, biomass, and chlorophyll *a* concentration of phytoplankton and **(B)** abundance of heterotrophic protists in the study stations in September 2015.

(**Figures 8L,M**) clearly identified all three strains as *A. ostenfeldii*. The right anterior margin of plate 1' was straight. The shape of the anterior sulcal plate sa was slightly variable within all three strains. The majority of cells had a "door-latch" shaped sa plate but more "A-shaped" sa plates were also present (**Figures 8Q,R**).

Phylogeny

The phylogenetic analysis for *Alexandrium ostenfeldii* including three strains isolated in this study (H-2-A4, H-1-G8, and H-3-D4) revealed a tree with seven distinct phylogenetic groups. All three strains isolated in this study from the Argentine Sea formed a well-supported (ML 96%) monophyletic group within a larger cluster of sequences that consists of the groups 5, 6, and 7 (**Figure 9**). The three strains of *Alexandrium ostenfeldii* were identical in the sequence of the LSU-fragment analyzed. The dissimilarity with the next neighbors in the tree (group 5) was ∼0.5%. All other groups displayed a higher dissimilarity peaking at 2% for the isolate from the Bohai Sea in China. The phylogenetic placement of H-3-D10 (not shown) identified this strain as *Alexandrium catenella* (=group I of the former *A. tamarense/A. fundyense/A. catenella* species complex). The dissimilarity of H-3-D10 with group II of the former *A. tamarense/A. fundyense/A. catenella* species complex was in the range of 5%.

Phycotoxins in Field Samples

Paralytic shellfish poisoning toxins were detected in plankton net tows at stations 4, 15, 17, 21, and 33 at relatively low abundances ranging between 114.4 ng NT^{-1} at station 33 and 2593.8 ng NT^{-1} at station 17 (**Figure 10**). The toxin profiles were dominated by gonyautoxin-1 and -4 (GTX1/4) at stations 15, 17, and 21. In addition to GTX1/4, C1/2, and GTX2/3 were detected at almost the same relative abundances at all five stations (**Figure 10**).

Lipophilic toxins were present at low abundances during the expedition [**Figure 6**, gymnodimine A (GYM) is not shown]. Domoic acid (DA) was found only at stations 15 and 17 at abundances of 2.0 and 6.1 ng NT^{-1}, respectively. The second-least abundant phycotoxin was GYM, found only at station 3 at an abundance of 45.4 ng NT^{-1}. SPX-1 was found at stations 17, 21, and 33 at abundances ranging from 0.5 ng NT^{-1} at station 21 to 143.6 ng NT^{-1} at station 33. The most-dominant lipophilic toxin in terms of geographic distribution and abundance was PTX-2, which was detected at stations 4, 5, 15, 17, 21, and 33 at abundances ranging from 15.6 ng NT^{-1} at station 5 to 5684.4 ng NT^{-1} at station 21.

Toxin Profiles of *Alexandrium* Isolates

The toxin profile of *Alexandrium catenella* strain H-3-D10 was dominated by C1/2 (72%), followed by GTX1/4 (15%), neosaxitoxin (NEO, 9%), GTX2/3 (2%), and saxitoxin (STX, 2%) (**Figure 11**). Also, the three *A. ostenfeldii* strains H-1-G8, H-3-D4, and H-2-A4 were producers of PSP toxin with a quantitatively different PSP profile than *A. catenella* H-3-D10. In contrast to

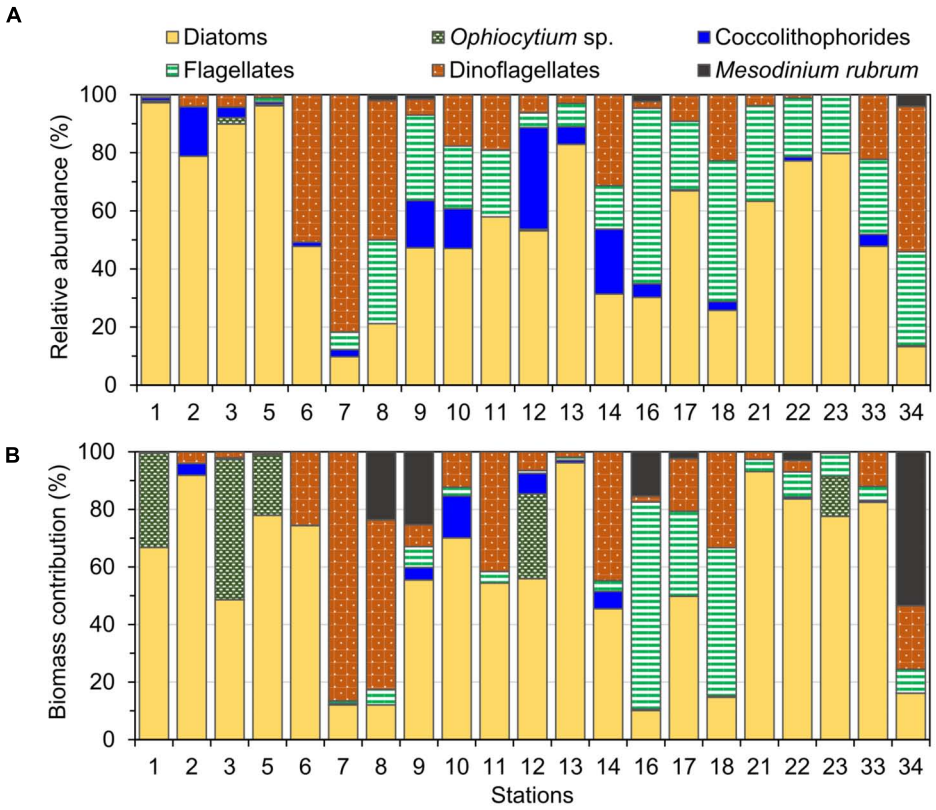

FIGURE 4 | Relative **(A)** abundance and **(B)** biomass of the main phytoplankton groups identified at the study stations in September 2015.

A. catenella, the most abundant toxins of the three *A. ostenfeldii* strains were GTX2/3 followed by C1/2 and STX (**Figure 11**).

In addition to PSP toxins, the three *A. ostenfeldii* strains also produced spirolides (**Figure 12**). The most-abundant spirolide among all three strains was SPX-1 ranging between 83 and 93% of total spirolides, followed by a novel spirolide with the pseudo-molecular $[M + H]^+$ ion *m/z* 592 ranging between 3.5 and 11.5%, which was named here spirolide M. All three *A. ostenfeldii* strains additionally contained five further spirolides as minor compounds: 27-hydroxy-13-desmethyl spirolide C and four, yet, uncharacterized spirolides named compounds (1) to (4) (**Figures 11**, **12**).

DISCUSSION

Environmental Conditions and Distribution of Plankton

The variability of hydrographic conditions in El Rincón has been ascribed to the seasonal influence of water mass currents along the shelf and shelf breakfronts, river discharges into the shallow area, and anthropogenic activities along the coastline (e.g., Lucas et al., 2005; Palma et al., 2008). In this study, the lower temperature and salinity registered at middle-shelf resulted from the influence of colder Subantarctic shelf waters diluted by low salinity discharges from the Magellan Strait (Palma and Matano, 2012), while the higher water temperatures in the shallow area of El Rincón were due to the northward outflow of high salinity and warmer waters from the San Matías Gulf into the inner-shelf (Palma et al., 2008). The freshwater discharges of the Negro and the Colorado Rivers (Lucas et al., 2005) were detected *in situ* at the coastal stations near their deltas, while the influence of the highly eutrophic and hypersaline Bahía Blanca Estuary (Guinder et al., 2010; López Abbate et al., 2015) was notable at stations 1 and 12, where the *in situ* salinities reached the maxima. A particular characteristic of El Rincón area is the formation of an anticyclone gyre in the center during winter, which looses intensification when nearing spring and summer (Palma et al., 2008). Lower concentrations of phytoplankton were found in the center of El Rincón, where the anticyclone gyre developed. Conversely, the growth of large diatoms with high carbon biomass at most coastal stations might be related with nutrient inputs from land such as the Bahía Blanca Estuary (Guinder et al., 2010; Koppprio et al., 2017; López Abbate et al., 2017) as well as with the mixed and turbid water column (Litchman and Klausmeier, 2008) characteristic of this shallow area (Guinder et al., 2009; Delgado et al., 2015). In eutrophic estuaries and adjacent coastal shelves, diatoms commonly dominate the phytoplankton, and this group is of high nutritional quality and facilitates efficient trophic transfer to support the secondary production (Winder et al., 2017). Dinoflagellates, the second-most abundant phytoplankton group in the area and dominant at the stratified middle-shelf

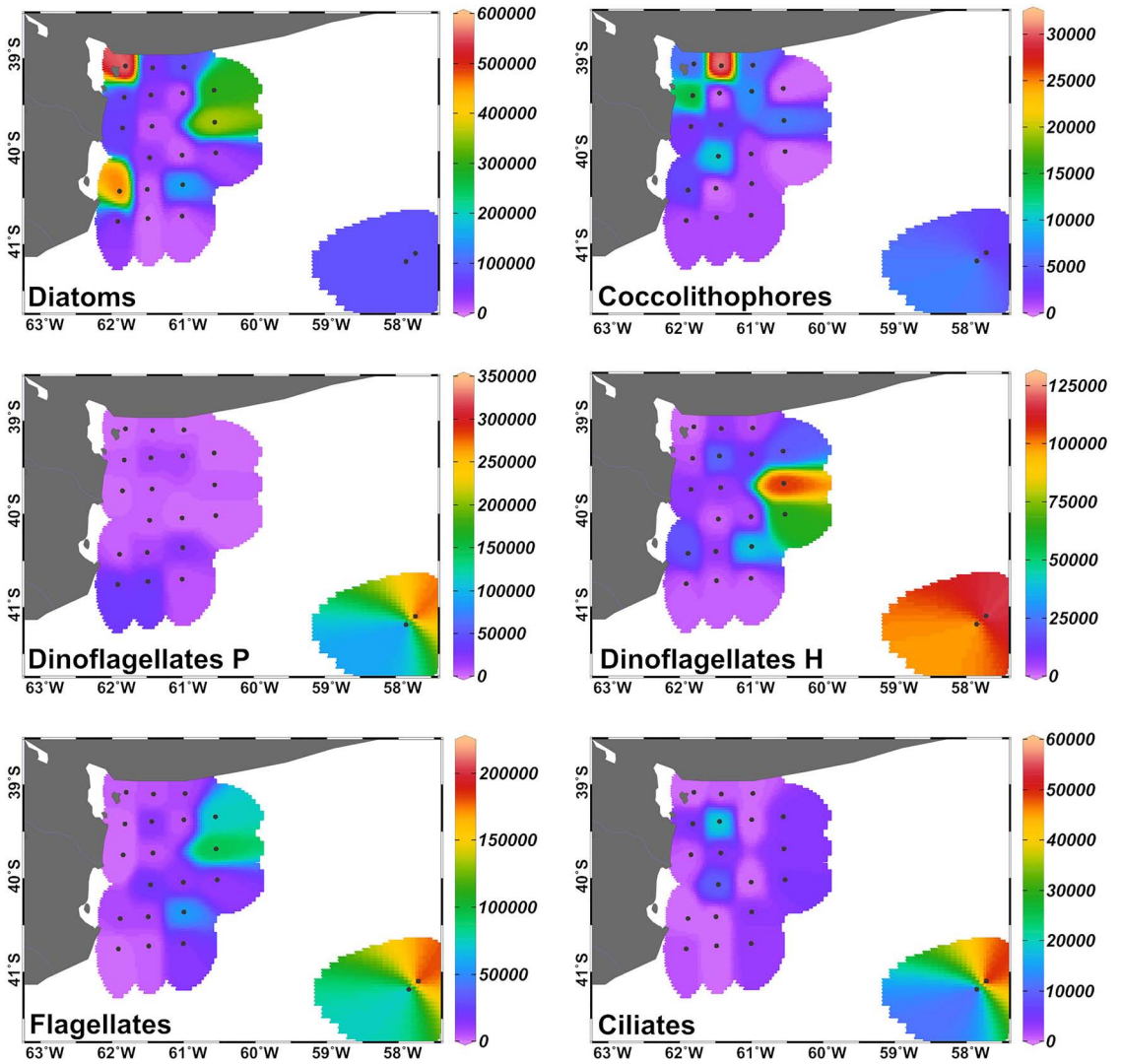

FIGURE 5 | Distribution of the abundance (in cells L^{-1}) of the main protists' groups (cells >5 μm) in the inner-shelf and at the two middle-shelf stations in September 2015. Dinoflagellates P: phototrophic, dinoflagellates H: heterotrophic.

stations (e.g., Carreto et al., 2016) also represent high food quality for higher trophic levels (Winder et al., 2017), except if they are toxigenic species (see section Lipophilic Toxins and Potential Producers in Field Samples). The high concentrations of heterotrophic protists (dinoflagellates and ciliates) at the middle-shelf might be related with an earlier phytoplankton bloom followed by zooplankton grazing (García et al., 2008; Carreto et al., 2016). Some particular species of dinoflagellates such as *Scrippsiella* sp. and *Heterocapsa* sp. were abundant at the coastal stations close to the Bahía Blanca Estuary (stations 1 and 2) and sandy beaches (stations 12–13), where these species have been commonly registered and associated with mixed and highly turbid waters (e.g., Guinder et al., 2010; Delgado et al., 2018). Similarly, the dinoflagellate *Prorocentrum minimum* was frequently found at several shallow stations of El Rincón, in agreement with the detection of this species blooming in weak stratified subantarctic waters (Gómez et al., 2011). Further, coccolithophore species, tintinnids, and naked ciliates also displayed differential distribution across the coastal middle-shelf transition, likely related to their specific ecological traits under different environmental conditions (*e.g.*, Le Quéré et al., 2005; Litchman and Klausmeier, 2008).

Considering that remote sensing chlorophyll data are often used as a proxy of phytoplankton biomass (Delgado et al., 2015), it is worth noting that in this study, abundance (in cells L^{-1}) and biomass (cell carbon content in μg C L^{-1}) of phytoplankton were only weakly correlated with chlorophyll. This might be related with the relatively high abundance of pico- and ultra-phytoplankton (<5 μm) characteristic of El Rincón (Negri et al., 2013), but it was not measured in this study and with the adjustment of the cell content of chlorophyll to fluctuating turbidity and underwater light conditions typical

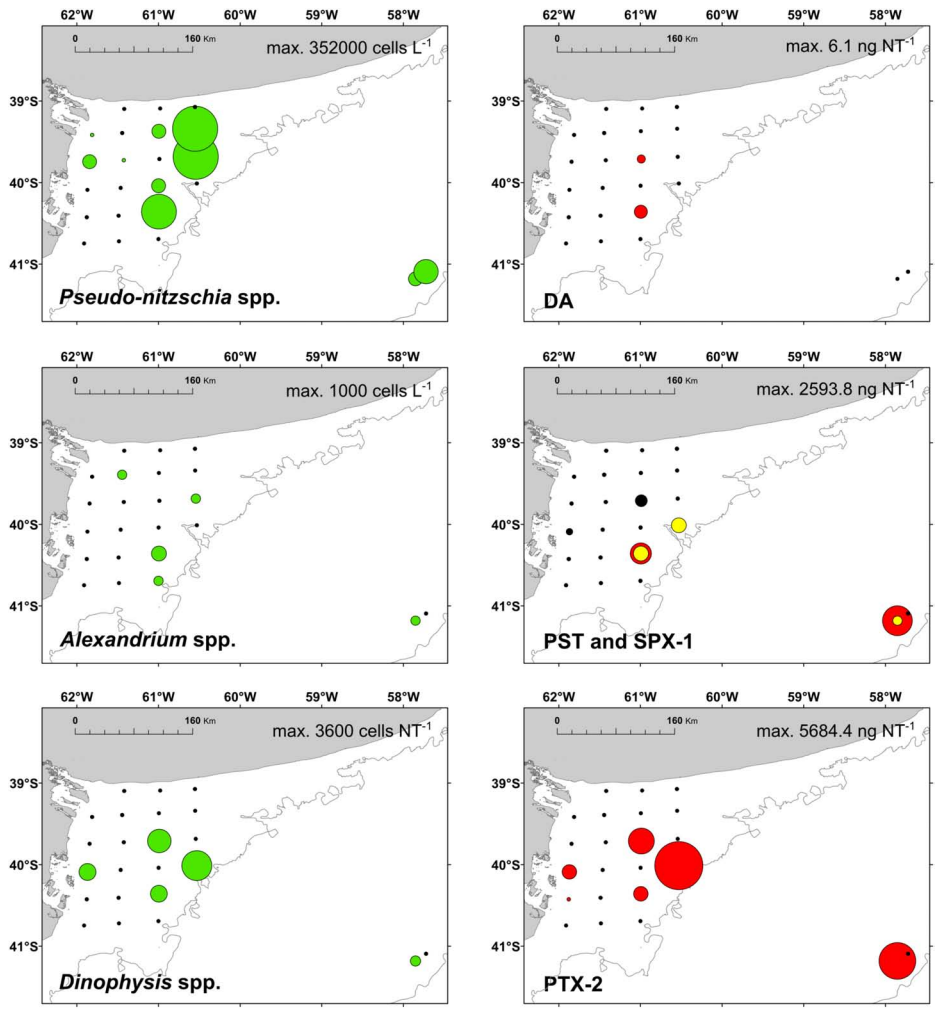

FIGURE 6 | Left panels: distribution of the potential toxigenic diatom *Pseudo-nitzschia* spp. and the dinoflagellate *Alexandrium* spp; and the ciliate *Mesodinium rubrum* (prey of *Dinophysis* spp.) (green); right panels: distribution of the respective phycotoxins in September 2015 (red). DA, domoic acid; PST, paralytic shellfish toxins; SPX-1, 13-desmethyl spirolide C (yellow); and PTX-2, pectenotoxin-2 (produced by *Dinophysis*).

of this coastal area (Guinder et al., 2009; Delgado et al., 2018).

Lipophilic Toxins and Potential Producers in Field Samples

In the present study, in agreement with historical records (Carreto et al., 1981), the detection of phycotoxins and their producers indicates the occurrence of HABs in a highly productive area of the Argentine shelf causing potential risk for marine biota and human welfare. The spatial heterogeneity of El Rincón seems to provide multiple niches for the development of diverse phytoplankton ecological traits including the production of toxins. Even in late winter, a number of lipophilic toxins were detected during the cruise. The amino acid domoic acid (DA) is produced by several species of the diatom of genera *Nitzschia* and *Pseudo-nitzschia* (Trainer et al., 2012). Here, blooms of *Pseudo-nitzschia* spp. were identified, but the low detection of domoic acid in the field could be related to the high species richness of this genus in the Argentine Sea (∼39–47°S), where half of them are non-toxigenic species (four of a total of eight described species; Almandoz et al., 2017). Identification of *Pseudo-nitzschia* up to species level by light microscopy is hardly possible and thus a correlation of *Pseudo-nitzschia* and DA is difficult. Furthermore, environmental factors influence the production of DA in *Pseudo-nitzschia*. A recent study has shown that DA production in a *Pseudo-nitzschia* species previously regarded as non-toxic was induced by the presence of herbivorous copepods (Harðardóttir et al., 2015). Additionally, mismatch between *Pseudo-nitzschia* and DA in the field samples could rely also on the sampling scheme. Samples for toxin analysis were obtained by horizontal plankton net tows, while cell counts were performed on Niskin bottle samples from discrete depth.

The most abundant toxin was PTX-2, which is produced by several species of the genus *Dinophysis* (Reguera et al., 2014). No cells of *Dinophysis* were detected in bottle samples

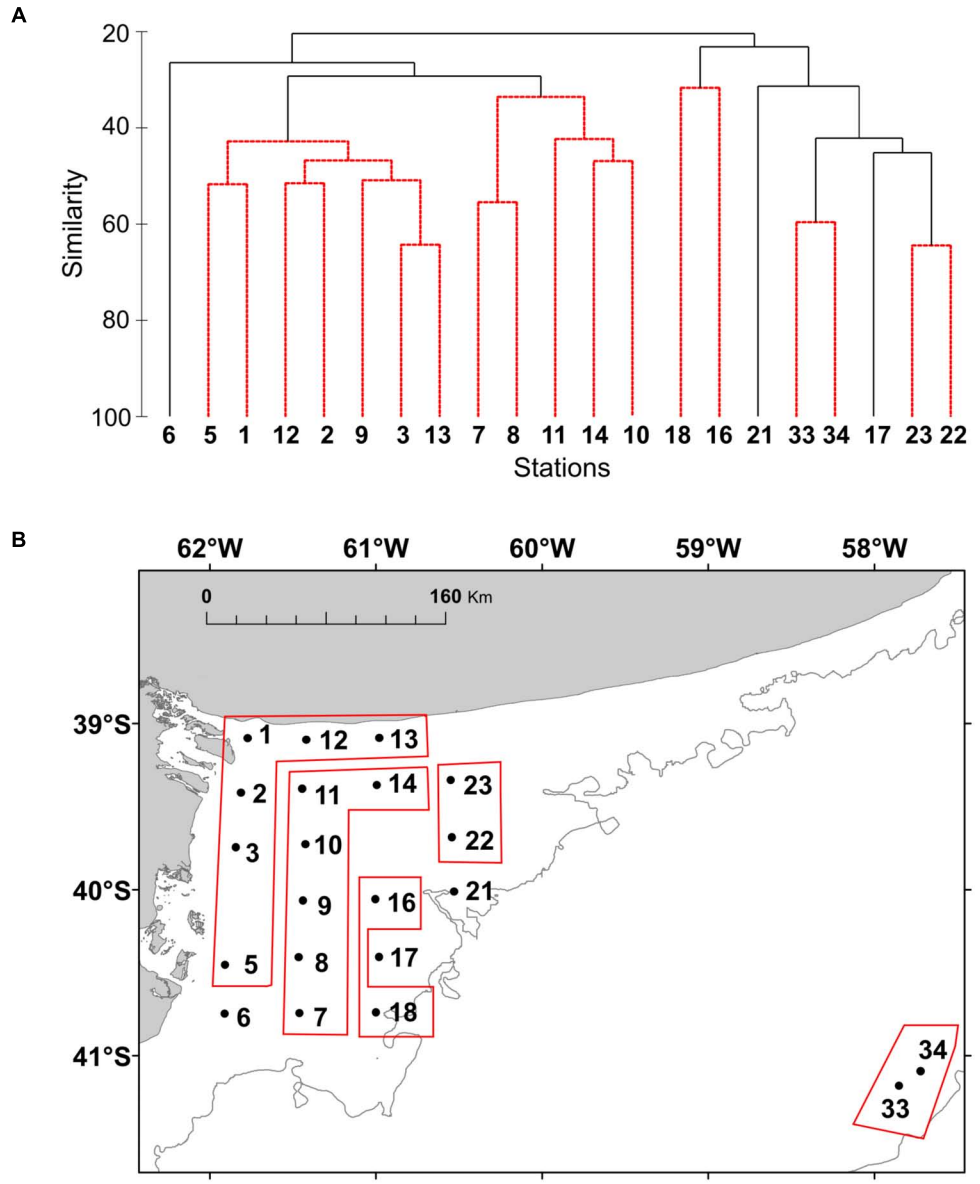

FIGURE 7 | (A) Cluster analysis based on Bray-Curtis similarity index of the plankton community at the study stations of El Rincón in September 2015.The abundance of the species (cells L^{-1}) was transformed using log (x + 1). **(B)** The resulted groups from the SIMPROF are shown in the map of the study area.

indicating an overall abundance below the detection limits of the sedimentation counting method. In the horizontal net samples, however, cells of *D. tripos*, and some of *D. acuminata* only at station 15, were found in co-occurrence with PTX-2 (**Figure 6**). A comparable link of *Dinophysis tripos* with PTX-2 was found by Fabro et al. (2015) in the Argentine Sea (∼38–56°S) in late summer, albeit at higher cell abundances and lower concentration of PTX-2 compared to this study. In late winter, potential predators of *Dinophysis,* such as *Noctiluca scintillans* and *Gyrodinium* spp., were also found abundant in net samples, especially at stations 17 and 21. Moreover, *Dinophysis* generally co-occurred with the ciliate *Mesodinium rubrum*, the obligate prey of this dinoflagellate (Park et al., 2006), which indicates potentially good growth conditions for *Dinophysis*. The dinoflagellate genus *Alexandrium* was found in relatively low abundance in the field. Cells of *Alexandrium* spp. were found in the shallow area of El Rincón and at the two middle-shelf stations. This is in agreement with previous studies that documented a wide distribution of the genus under contrasting physical conditions at a wide latitudinal range of the Argentine shelfbreak front (Carreto et al., 1998; Montoya et al., 2010; Almandoz et al., 2014; Fabro et al., 2017). The presence of cells of *Alexandrium* spp. in the field was related with the detection of PSP toxins, in particular, *A. ostenfeldii* and the spirolide SPX-1 (**Figure 6**). Furthermore, the most abundant toxins produced by the *Alexandrium* isolates (C1/2,

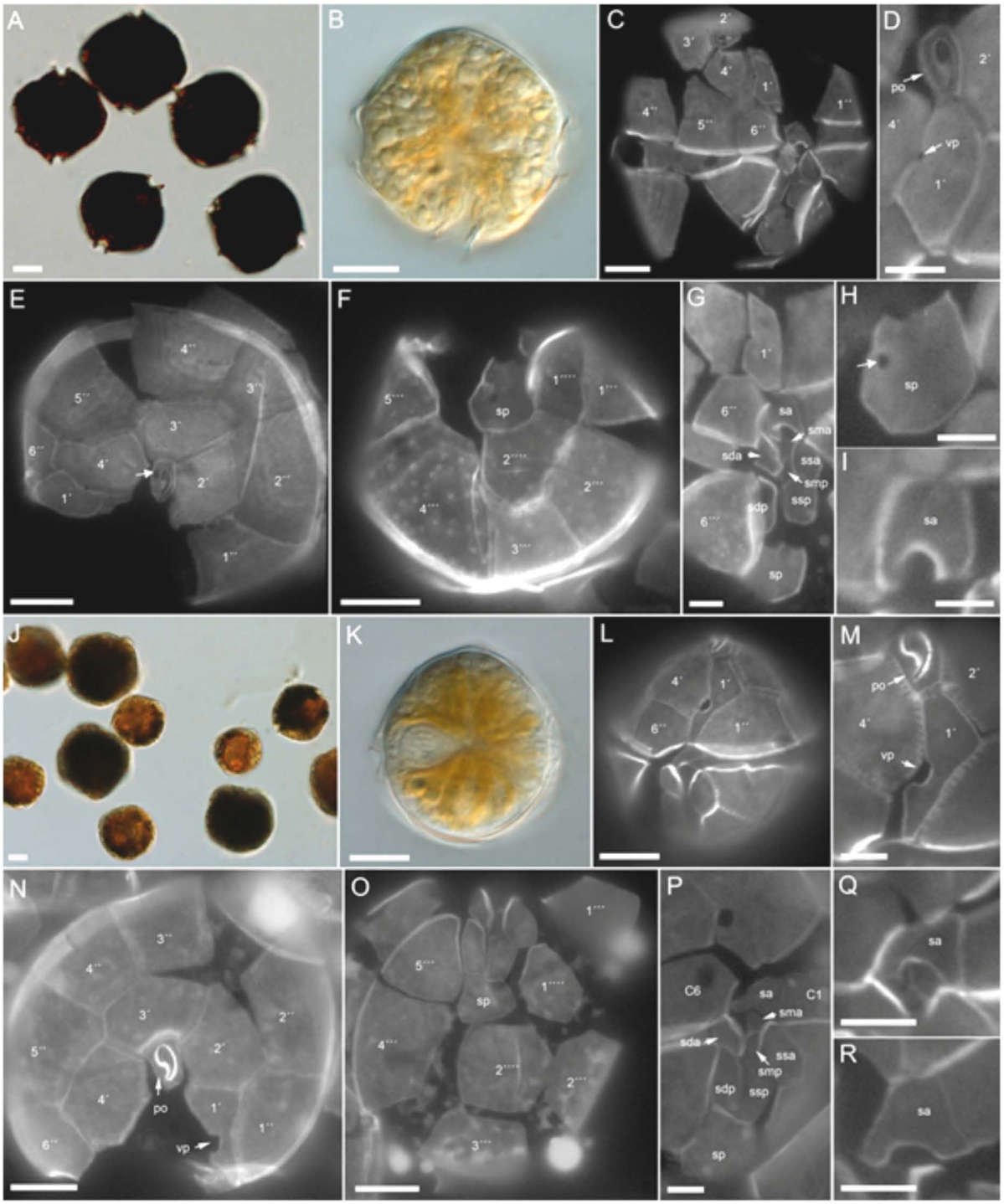

FIGURE 8 | *Alexandrium* spp. morphology. **(A–I)** *A. catenella* (H3-D10). Bright field images of **(A)** lugol-stained or **(B)** living cell. Epifluorescence images of calcofluor-stained cells showing **(C–G)** the plate pattern, and **(H)** details of the posterior and **(I)** anterior sulcal plate. Note in **(D)** the ventral pore (vp) and in **(E)** the attachment pore on the pore plate (white arrow). **(J–R)** *A. ostenfeldii* (H-3D4). Bright field images of **(J)** lugol-stained or **(K)** living cell. Epifluorescence images of calcofluor-stained cells showing **(L–P)** the plate pattern, and **(Q,R)** details of the anterior sulcal plate. Vp, ventral pore; Po, pore plate. Plate labels according to the Kofoidean system. Sulcal plates abbreviations: sp, posterior sulcal plate; ssp, left posterior sulcal plate; sdp, right posterior sulcal plate; smp, median posterior sulcal plate; sda, right anterior sulcal plate; ssa, left anterior sulcal plate; sma, median anterior sulcal plate; sa, anterior sulcal plate. Scale bars = 10 μm **(A–C,E,F,J–L,N,O)** or 5 μm **(D,G–I,M,P–R)**.

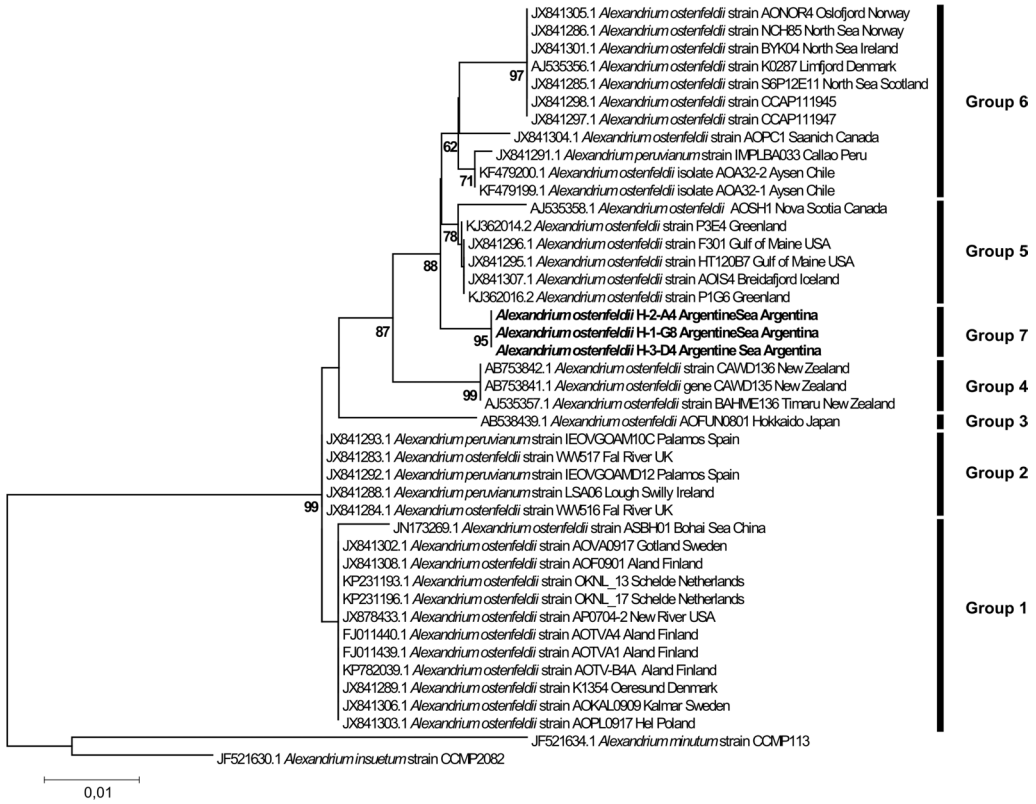

FIGURE 9 | Phylogenetic tree of *Alexandrium ostenfeldii*.

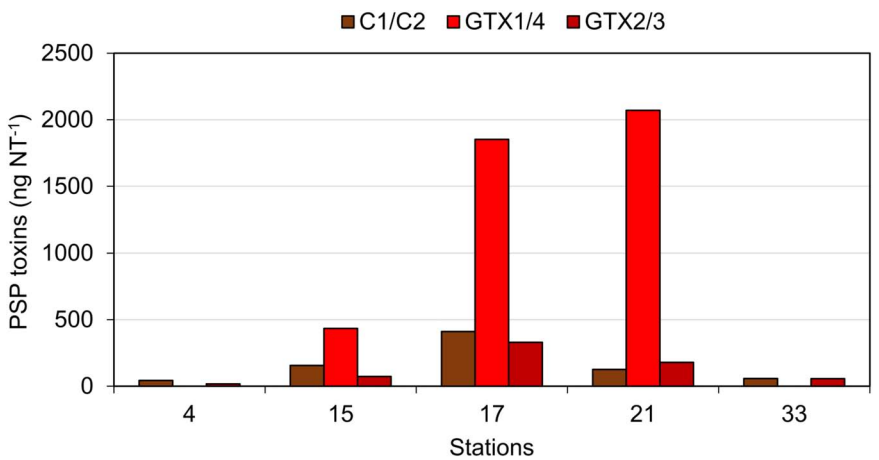

FIGURE 10 | The PSP toxins detected in net hauls of plankton. Note that the water columns sampled at different stations were not normalized and quantitative comparisons among stations are not possible.

GTX2/3, and SPX-1) were also detected in the samples of plankton.

Phylogeny of *Alexandrium* Strains

In the Argentine Sea, the genus *Alexandrium* has been registered in a wide latitudinal area (∼37–55.5°S) either near the coast, middle-shelf, and shelfbreak front, not only mainly in spring, but also in autumn and summer (e.g., Balech, 1995; Carreto et al., 1998; Gayoso and Fulco, 2006; Montoya et al., 2010). Most of the species identified by microscopy and/or molecular analyses belong to the *A. tamarense/catenella/fundyense* complex (Fabro et al., 2017 and references therein). In previous studies, there was only one strain of the *A. tamarense/catenella/fundyense* species complex isolated from the Argentine shelf that has

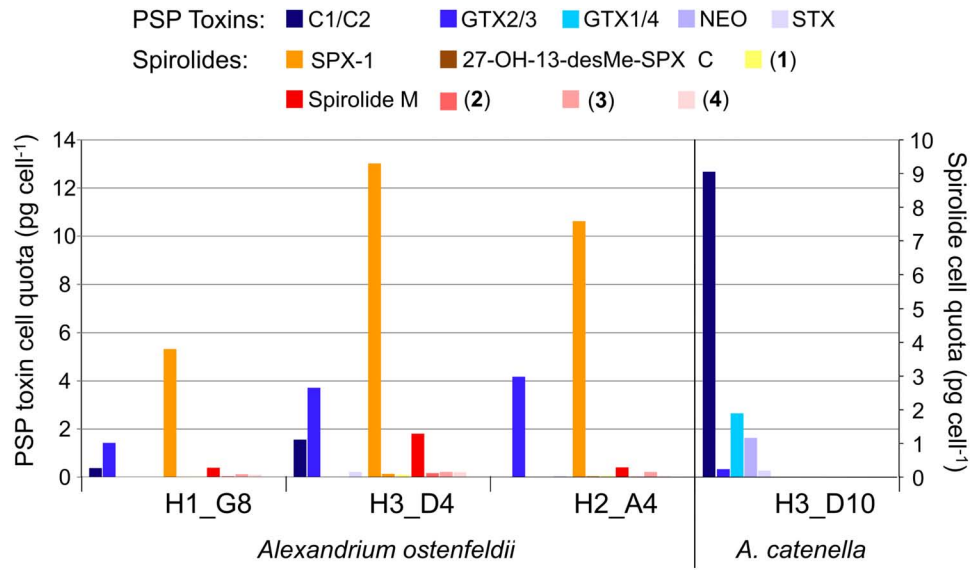

FIGURE 11 | Profiles of the toxin of four *Alexandrium* isolates.

been genetically characterized and identified as ribotype group I (which now in the new nomenclature of the genus is *A. catenella*), that is, the strain MDQ1096 isolated from the coast of Mar del Plata (∼38°S), 500 km north of the Bahía Blanca Estuary (Carreto et al., 2001; Penna et al., 2008). In addition, the sequence analyses of the two strains, H5 and H7, isolated from the San Jorge Gulf (∼45–47.5°S) in autumn 2012, and reported in the old morphological terminology as *A. tamarense* by Krock et al. (2015), are now confirmed to be *A. catenella*, that is, ribotype group I of the *A. tamarense/catenella/fundyense* species complex (Metfies and Tillmann, unpublished). Genetic analysis has shown that the strain MDQ1096 has the same D1–D2 LSU rRNA gene sequences as the *A. catenella* from Chilean waters and from the Southeast Pacific (Lilly et al., 2007; Aguilera-Belmonte et al., 2011). All these studies carried out in the Argentine continental shelf over the last decades support the apparent dominance of *A. catenella* over other *Alexandrium* species in that area and further suggest that its population reaches wide distribution in the Southern Hemisphere.

The new sequence data of the Argentine Sea *Alexandrium ostenfeldii* strains in the LSU phylogenetic analysis added a new and well-supported ribotype group to the six groups identified previously (Kremp et al., 2014; Salgado et al., 2015; Van de Waal et al., 2015). The general clustering of the sequences is in agreement with previous phylogenetic analyses based on concatenated rDNA (Orr et al., 2011; Kremp et al., 2014) with two main clusters, where groups 1 and 2 are forming one cluster and the other groups are forming another cluster. Groups 1 and 2 subsume strains from various parts of the globe with all strains from group 1 originating from low-salinity environments. Strains of group 2 originate from coastal embayments and estuaries of Ireland, the United States, and the Spanish Mediterranean. In contrast, grouping of strains in groups 3–7 seems to match their geographic distribution, with group 3 representing Japan, group 4 from New Zealand, and group 5 with strains from the North Atlantic up to the Greenland coast. For strains currently unified in group 6, a further substructure into a clade with strains from the North Sea (including adjacent fjords as Oslofjord and Limfjord) and another clade with strains from the South Pacific (Chile, Peru) is indicated, but only weakly statistically supported by a bootstrap value of 61. The separate placement of our first Argentinean *A. ostenfeldii*, representing the first data from the South Atlantic, perfectly fits into such a picture of geographically separated *A. ostenfeldii* populations.

PSP Toxin Profiles in Field Samples and Toxin Profiles of *Alexandrium* Isolates

It is noteworthy that the quantitative field profiles of the PSP toxin did not match the relative abundance of PSP toxins of the *Alexandrium* strains isolated during this expedition. The PSP profiles of all three *A. ostenfeldii* strains were dominated by GTX2/3, whereas the PSP profile of the *A. catenella* strain was dominated by C1/2. In contrast, the profiles of the toxin of stations 15, 17, and 21 were dominated by GTX1/4. The GTX1/4 were not detected at station 33, but only C1/2 and GTX2/3 were detected (**Figure 10**). However, it is reasonable to assume that GTX1/4 was present, but not detected as its limit of detection (LOD) is much higher than the LOD of C1/2 and GTX2/3. The GTX1/4 were only produced by the *A. catenella* strain, but at a lower abundance as C1/2. This toxin profile is consistent with profiles previously reported of *A. catenella* in the region (Montoya et al., 2010; Krock et al., 2015). Interestingly, the discrepancy between the profiles of the PSP toxin of isolated strains and that of the field samples of the plankton in the Argentine Sea observed here (**Figures 10**, **11**) has been seen previously (Montoya et al., 2010) and may indicate either a

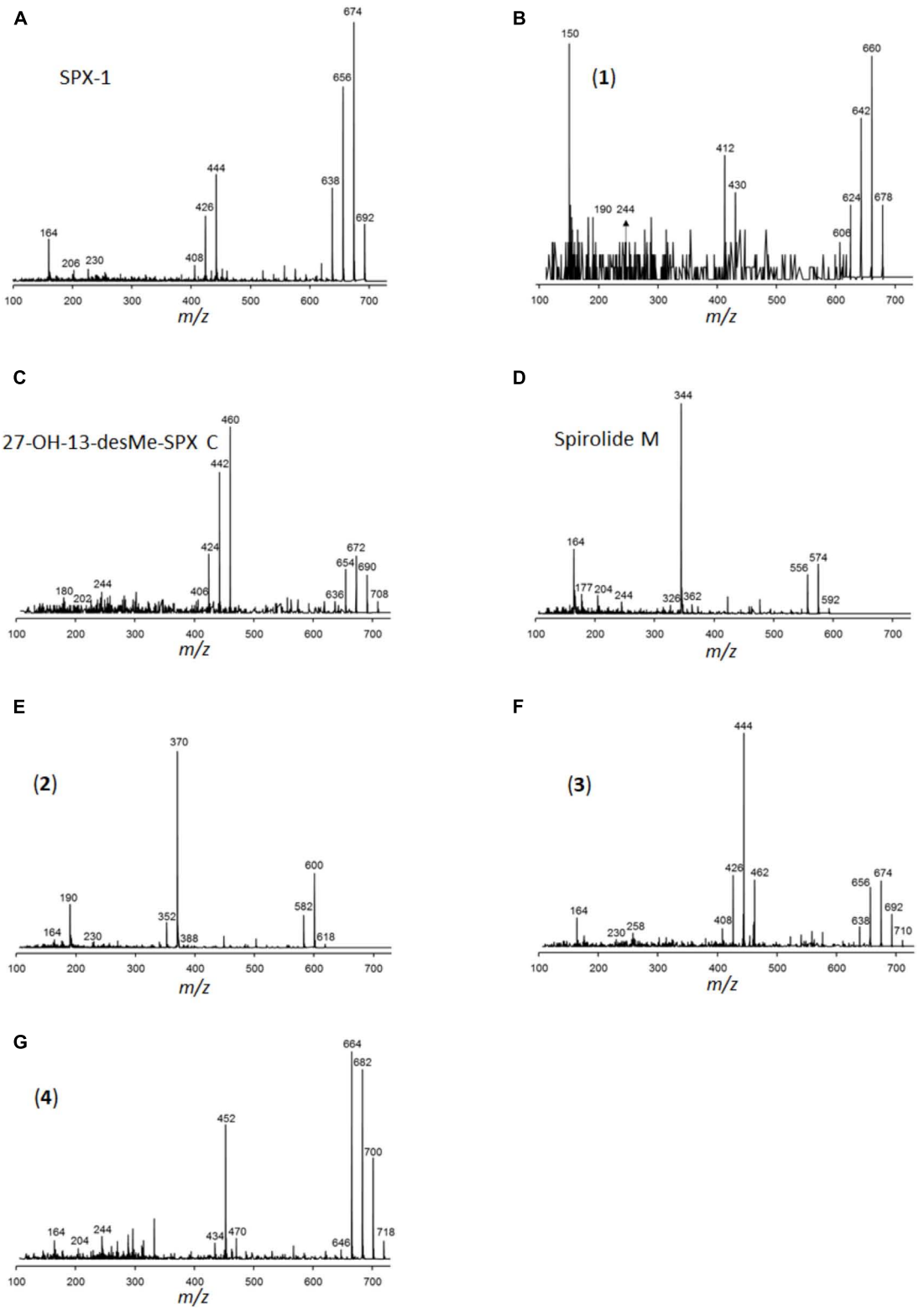

FIGURE 12 | Collision-induced dissociation (CID) spectra of the spirolides detected in *A. ostenfeldii*: **(A)** SPX-1 (13-desMethyl-spirolide C), identical with spectrum shown in Sleno and Volmer (2005), **(B)** 13/19,31-didesMethyl-spirolide C, **(C)** 27-Hydroxy-13-desMethyl-spirolide C, **(D)** Spirolide M, **(E)** compound 2, **(F)** compound 3, and **(G)** compound 4.

change in production of toxins in relation to growth conditions of the culture or may be related with an unexplored diversity of PSP-producing organisms in the SW Atlantic. There are few previous reports of the toxin profiles of *A. ostenfeldii* of the SW Atlantic. The presence of *A. ostenfeldii* at higher latitudes of the Patagonian shelf has been well known for a long time (Balech, 1995), and this has been recently reaffirmed (Fabro et al., 2017), but no strains were isolated for toxinological studies. The only available strain to compare our data with is an *A. ostenfeldii* strain isolated from the Beagle Channel (54° S) (Almandoz et al., 2014) that did not produce PSP toxins, but only spirolides. In addition to the lack of production of PSP of the strain from the Beagle Channel (BC), the profiles of the spirolide of the BC strain and the three strains of this expedition were quite different: the BC strain was reported to produce SPX-1, 20-methyl spirolide-G and an unknown spirolide with *m/z* 592, whereas the three strains investigated in this work produced SPX-1 [retention time (RT) 12.3 min], 27-hydroxy-13-desmethyl spirolide-C (RT 12,6 min), spirolide-M (RT 12.7 min), and four undescribed spirolides (**Figure 11**). The only common spirolides in strains from both areas are SPX-1 and spirolide-M with *m/z* 592 (see in the following). The CID spectrum of the unknown spirolide *m/z* 592 reported by Almandoz et al. (2014) and spirolide-M show identical fragments (**Figure 12D**; Almandoz et al., 2014). Moreover, the chromatographic behavior of spirolide-M and the unknown *m/z* 592 is consistent as both compounds elute after SPX-1, which in addition to the mass spectrometric data is a strong evidence that spirolide-M is also present in the BC strain.

Description of Novel Spirolides

The three *A. ostenfeldii* strains isolated from the Argentine shelf produced five novel spirolides, which highlights the large structural variability of this class of toxin. Compound (1) (*m/z* 678, RT 11.9 min) shares its molecular mass and most fragments of the CID spectrum with 13,19-didesmethyl spirolide C (13,19-didesMe SPX C). An obvious difference between both CID spectra is the cycloimine fragment, which is *m/z* 164 in the case of 13, 19-didesMe SPX C and *m/z* 150 in the case of compound (**1**). The fragment *m/z* 150 is typical for A-type spirolides that are lacking the methyl group at C31 (Hu et al., 2001). Given this evidence, it is reasonable to assume that the missing methyl group at C31 is located at a different position such as C13 or C19 that are often methylated in spirolides. However, the exact position of the shifted methyl group cannot be determined by mass spectrometry alone.

With the pseudo-molecular $[M + H]^+$ ion *m/z* 592, spirolide M (SPX M) is the smallest yet reported spirolide. The difference of the mass in comparison with the next bigger spirolide (spirolide H, *m/z* 650; Roach et al., 2009) is 58 Da. In comparison with the CID spectrum of spirolide H (SPX H), only two water losses from the pseudo-molecular ion are observed (*m/z* 574 and 556) instead of three in the CID spectrum of SPX H. The difference in the mass between the $[M + H]^+$ ion and the midmass fragment of SPX M is 248 Da (*m/z* 592 > 344), which is typical for spirolides of the C-type and SPX H. The loss of 248 Da is clear evidence that the C1-C11 part of SPX M must be identical to SPX H. Additionally, the spectrum of SPX M shows the identical small fragments of the cycloimine moiety (*m/z* 164, 177, and 204), which leads to the conclusion that the cycloimine ring with its five adjacent C atoms is also identical to SPX H. However, the CID spectrum of SPX M displays a fragment *m/z* 244 that is 14 Da higher than the fragment *m/z* 230 of SPX H. These mass spectral elements are consistent with a structure identical to SPX H with the difference of SPX M containing a dimethylated monospiroketal ring instead of the dispiroketal ring system of SPX H. However, most spirolides possess trispiroketal ring systems; only SPX H and I have dispiroketal ring systems. In contrast, SPX M is the first spirolide to be reported to have only a monospiroketal ring.

The difference in mass of compound **(2)** (*m/z* 618, RT 13, 6 min) to the closest known spirolide in terms of molecular mass SPX H is 32 Da. Similar to SPX M, compound (**2**) also eliminates 248 Da from its $[M + H]^+$ ion, which indicates a conserved structure in the C1-C11 part of the spirolide such as SPX C and H. However, the CID spectrum of compound (**2**) shows a fragment *m/z* 190, which has not been observed in other spirolides. Most spirolides form a *m/z* 164 fragment or a *m/z* 180 fragment in the case of a 27-hydroxylation. However, a fragment *m/z* 190 has not been observed in spirolides and thus it is difficult to interpret without additional information.

Compound **(3)** has the pseudo-molecular ion of *m/z* 710 (RT 12.50 min) and differs from the previous spirolides by a mass difference of 266 Da (instead of 248 Da) between the $[M + H]^+$ ion and the midmass fragment *m/z* 462. This cleavage has not been detected in other spirolides, but can be explained by a hydroxylation and a reduction of a double bond between positions C1-C11. These hypothetical changes applied to SPX-1 would in fact result in a pseudo-molecular ion *m/z* 710. Nevertheless, there still must be other structural differences between SPX-1 and compound (**3**), because compound (**3**) produces the fragments m/z 230 and 258, which are not observed in the CID spectrum of SPX-1. Fragment *m/z* 258 is also formed by 20-methyl spirolide G, which has a 6-6-5 trispiroketal ring system instead of the 6-5-5 trispiroketal ring system of most other spirolides. An exact structure of compound (**3**) cannot be assigned by mass spectral data alone.

Compound **(4)** shows a pseudo-molecular ion of *m/z* 718 (RT 13.0 min) differing from compounds (**1–3**) by a mass difference of 266 Da between the $[M + H]^+$ ion and the midmass fragment *m/z* 452. Accordingly, it can be deduced that compounds (**3**) and (**4**) share the same structural element between positions C1-C11. These changes applied to SPX-1 would result in a hypothetical pseudo-molecular ion of *m/z* 710, which is 8 Da less than the actual observed ion *m/z* 718. Since the cycloimine fragments *m/z* 164 and 204 are conserved in (**4**), identical structures of the cycloimine moiety between SPX-1 and compound (**4**) can be deduced. This means that an additional structural difference between SPX-1 and compound (**4**) must be located in the trispiroketal ring system. Full structural elucidation of the novel compounds can only be achieved by NMR spectroscopy that was not applicable in this case, because of the need for purified compounds in the microgram range, which was impossible to achieve within this study.

FINAL REMARKS

So far, this is the first study in the shelf area of El Rincón that contemplates in detail the composition and the structure of the plankton community >5 μm, including phototrophic and heterotrophic protists. Under the growing need for the global plankton register to assess community changes and their underlying drivers, our study provides baseline information of plankton state in a highly productive area of the Global Ocean. Moreover, our work highlights the necessity of combining complementary approaches in plankton studies to address the diversity and distribution of the potential toxic species. Morphological differentiation between the species of the former *Alexandrium tamarense/fundyense/catenella* complex is impossible and molecular sequencing is inevitable in this case to facilitate species identification. Further integrative studies of toxin production are needed to fully evaluate the discrepancy between phycotoxin profiles quantified in the field and in isolated cells grown in the laboratory. Our findings reinforce the presence of toxigenic species in the Argentine shelf, indicating a possible hazard for fisheries and human well-being. The first molecular characterization of *A. ostenfeldii* for the SW Atlantic and the detection of novel spirolides suggest that the Patagonian Shelf is still an extensive underexplored area of the Global Ocean.

AUTHOR CONTRIBUTIONS

VG, UT and BK designed the study. VG contributed to sampling, microscopic identifications and counting, data analyses and drafting the work. UT contributed to sampling, isolation, culturing, LM, and taxonomy of *Alexandrium* spp. BK and TK contributed to the LC-MS/MS analysis and interpretation of phycotoxins profiles. AD contributed to satellite image process and interpretation. JGC contributed to sampling and chlorophyll data. KM contributed to molecular analyses and interpretation. CLA and RS supported for microscopic identifications and editing. RL contributed to logistic support for sampling. All authors contributed with the interpretation of the results and have approved the final version.

FUNDING

This study was supported by the bilateral project MINCYT-DAAD (Ministerio de Ciencia, Tecnología e Innovación Productiva, Argentina and Deutscher Akademischer Austauschdienst, Germany), code DA/13/04; two research projects of Agencia Nacional de Promoción Científica y Tecnologica (ANPCyT), codes PICT-1681-2013 and PICT-1241-2013; the binational project MINCyT-BMBF (AL/11/03-ARG 11/021) and the Helmholtz-Gemeinschaft Deutscher Forschungszentren through the research program PACES of the Alfred-Wegener-Institut, Helmholtz-Zentrum für Polar- und Meeresforschung. Financial support for open-access publication was given by BMBF (Post Grant Fund # 16PGF0042).

SUPPLEMENTARY MATERIAL

The Supplementary Material for this article can be found online at: https://www.frontiersin.org/articles/10.3389/fmars.2018.00394/full#supplementary-material

REFERENCES

Acha, E. M., Ehrlich, M. D., Muelbert, J. H., Pájaro, M., Bruno, D., Machinandiarena, L., et al. (2018). "Ichthyoplankton associated to the frontal regions of the Southwestern Atlantic," in *Plankton Ecology of the Southwestern Atlantic, From Subtropical to the Subantarctic Realm*, eds M. Hoffmeyer, M. E. Sabatini, F. Brandini, D. Calliari, and N. H. Santinelli (Berlin: Springer), 219–246.

Acha, E. M., Mianzan, H. W., Guerrero, R. A., Favero, M., and Bava, J. (2004). Marine fronts at the continental shelves of austral South America. *J. Mar. Syst.* 44, 83–105. doi: 10.1016/j.jmarsys.2003.09.005

Aguilera-Belmonte, A., Inostroza, I., Franco, J. M., Riobó, P., and Gómez, P. I. (2011). The growth, toxicity and genetic characterization of seven strains of *Alexandrium catenella* (Whedon and Kofoid) Balech 1985 (Dinophyceae) isolated during the 2009 summer outbreak in southern Chile. *Harmful Algae* 12, 105–112. doi: 10.1016/j.hal.2011.09.006

Akselman, R., and Negri, R. M. (2012). Blooms of Azadinium cf. *spinosum* Elbrächter et Tillmann (Dinophyceae) in northern shelf waters of Argentina. Southwestern Atlantic. *Harmful Algae* 19, 30–38. doi: 10.1016/j.hal.2012.05.004

Almandoz, G. O., Fabro, E., Ferrario, M., Tillmann, U., Cembella, A., and Krock, B. (2017). Species occurrence of the potentially toxigenic diatom genus *Pseudo-nitzschia* and the associated neurotoxin domoic acid in the Argentine Sea. *Harmful Algae* 63, 45–55. doi: 10.1016/j.hal.2017.01.007

Almandoz, G. O., Ferrario, M. E., Ferreyra, G. A., Schloss, I. R., Esteves, J. L., and Paparazzo, F. E. (2007). The genus *Pseudo-nitzschia* (Bacillariophyceae) in continental shelf waters of Argentina (Southwestern Atlantic Ocean, 38-55 S). *Harmful Algae* 6, 93–103. doi: 10.1016/j.hal.2006.07.003

Almandoz, G. O., Montoya, N. G., Hernando, M. P., Benavides, H. R., Carignan, M. O., and Ferrario, M. E. (2014). Toxic strains of the *Alexandrium ostenfeldii* complex in southern South America (Beagle Channel, Argentina). *Harmful Algae* 37, 100–109. doi: 10.1016/j.hal.2014.05.011

Anderson, D. M., Alpermann, T. J., Cembella, A. D., Collos, Y., Masseret, E., and Montresor, M. (2012). The globally distributed genus *Alexandrium*: multifaceted roles in marine ecosystems and impacts on human health. *Harmful Algae* 14, 10–35. doi: 10.1016/j.hal.2011.10.012

Antoine, D. (2004). *Guide to the Creation and Use of Ocean-Colour, Level-3, Binned Data Products*. Reports of the International Ocean-Colour Coordinating Group No.4. Dartmouth, NS: IOCCG.

Balech, E. (1995). *The Genus Alexandrium Halim (Dinoflagellata)*. Cork: Sherkin Island, Co., 151.

Benavides, H., Prado, L., Diaz, S., and Carreto, J. I. (1995). "An exceptional bloom of *Alexandrium catenella* in the Beagle channel, Argentina," in *Harmful Marine Algal Blooms*, eds P. Lassus, G. Arzul, E. Erard-le Denn, P. Gentien, and C. Marcaillou-Le Baut (Paris: Lavoisier Intercept Ltd.), 113–119.

Bianchi, A. A., Ruiz Pino, D., Perlender, H. G. I., Osiroff, A. P., Segura, V., Lutz, V., et al. (2009). Annual balance and seasonal variability of sea-air CO2 fluxes in the Patagonia Sea: their relationship with fronts and chlorophyll distribution. *J. Geophys. Res.* 114:C03018. doi: 10.1029/2008JC004854

Bogazzi, E., Baldoni, A. N., Rivas, A., Martos, P., Reta, R. A., Orensanz, J. M., et al. (2005). Spatial correspondence between areas of concentration of Patagonian scallop (*Zygochlamys patagonica*) and frontal systems in the southwestern Atlantic. *Fish. Oceanogr.* 14, 359–376. doi: 10.1111/j.1365-2419.2005.00340.x

Brown, O. B., and Minnet, P. J. (1999). *MODIS Infrared Sea Surface Temperature Algorithm*. Technical Report No ATBD25. Coral Gables, FL: University of Miami.

Campbell, J. W., Blaisdell, J. M., and Darzi, M. (1995). "Level-3 SeaWiFS data products: spatial and temporal binning algorithms," in *NASA Technical Memorandum 1995-104566*, Vol. 32, eds S. B. Hooker, E. R. Firestone, and J. G. Acker (Greebelt, MD: SeaWiFS Technical Report Series; NASA-GSFC), 1–73.

Carranza, M. M., Gille, S. T., Piola, A. R., Charo, M., and Romero, S. I. (2017). Wind modulation of upwelling at the shelf-break front off Patagonia: observational evidence. *J. Geophys. Res. Oceans* 122, 2401–2421. doi: 10.1002/2016JC012059

Carreto, J. I., Akselman, R., Montoya, N. G., Negri, R. N., Benavides, H., Carignan, M. O., et al. (1998). "*Alexandrium tamarense* blooms and shellfish toxicity in the Argentine Sea: a retrospective view," in *Proceedings of the VIII International Conference on Harmful Algae*, eds B. Reguera, J. Blanco, M. L. Fernández, and T. Wyatt (Vigo), 131–134.

Carreto, J. I., Carignan, M. O., and Montoya, N. G. (2001). Comparative studies on mycosporine-like amino acids, paralytic shellfish toxins and pigment profiles of the toxic dinoflagellates *Alexandrium tamarense*, *A. catenella* and *A. minutum*. *Mar. Ecol. Progr. Ser.* 223, 49–60. doi: 10.3354/meps223049

Carreto, J. I., Lasta, M., Negri, R. M., and Benavides, H. R. (1981). *Los Fenómenos de Marea Roja y Toxicidad de Moluscos Bivalvos en el Mar Argentino*. Mar del Plata: INIDEP, 399.

Carreto, J. I., Montoya, N. G., Carignan, M. O., Akselman, R., Acha, E. M., and Derisio, C. (2016). Environmental and biological factors controlling the spring phytoplankton bloom at the Patagonian shelf-break front-Degraded fucoxanthin pigments and the importance of microzooplankton grazing. *Prog. Oceanogr.* 146, 1–21. doi: 10.1016/j.pocean.2016.05.002

Clarke, K. R., and Gorley, R. N. (2006). *PRIMER v6: User Manual/Tutorial*. Plymouth: PRIMER E.

Delgado, A. L., Loisel, H., Jamet, C., Vantrepotte, V., Perillo, G. M., and Piccolo, M. (2015). Seasonal and inter-annual analysis of chlorophyll-a and inherent optical properties from satellite observations in the inner and mid-shelves of the south of buenos aires province (Argentina). *Remote Sens.* 7, 11821–11847. doi: 10.3390/rs70911821

Delgado, A. L., Guinder, V. A., Dogliotti, A., Zapperi, G., and Pratolongo, P. (2018) Consistency of MODIS-aqua(absorption)by phytoplankton coefficient in Southern Atlantic Ocean coastal optically complex waters: analysis and validation. Accepted in continental shelf Research.

Díaz, M. V., Marrari, M., Casa, V., Gattás, F., Pájaro, M., and Macchi, G. J. (2018). Evaluating environmental forcing on nutritional condition of *Engraulis anchoita* larvae in a productive area of the Southwestern Atlantic Ocean. *Prog. Oceanogr.* 168, 13–22. doi: 10.1016/j.pocean.2018.09.007

Dogliotti, A. I., Schloss, I. R., Almandoz, G. O., and Gagliardini, D. A. (2009). Evaluation of SeaWiFS and MODIS chlorophyll-a products in the argentinean patagonian continental shelf (38°-55°S). *Int. J. Remote Sens.* 30, 251–273. doi: 10.1080/01431160802311133

Fabro, E., Almandoz, G. O., Ferrario, M., John, U., Tillmann, U., Toebe, K., et al. (2017). Morphological, molecular, and toxin analysis of field populations of *Alexandrium* genus from the Argentine Sea. *J. Phycol.* 53, 1206–1222. doi: 10.1111/jpy.12574

Fabro, E., Almandoz, G. O., Ferrario, M., Tillmann, U., Cembella, A., and Krock, B. (2016). Distribution of *Dinophysis* species and their association with lipophilic phycotoxins in plankton from the Argentine Sea. *Harmful Algae* 59, 31–41. doi: 10.1016/j.hal.2016.09.001

Fabro, E., Almandoz, G. O., Ferrario, M. E., Hoffmeyer, M. S., Pettigrosso, R. E., Uibrig, R., et al. (2015). Co-occurrence of *Dinophysis tripos* and pectenotoxins in Argentinean shelf waters. *Harmful Algae* 42, 25–33. doi: 10.1016/j.hal.2014.12.005

Ferreira, A., Stramski, D., García, C. A., García, V. M., Ciotti, A. M., and Mendes, C. R. (2013). Variability in light absorption and scattering of phytoplankton in Patagonian waters: role of community size structure and pigment composition. *J. Geophys. Res. Oceans* 118, 698–714. doi: 10.1002/jgrc.20082

Franco, B. C., Palma, E. D., Combes, V., and Lasta, M. L. (2017). Physical processes controlling passive larval transport at the patagonian shelf break front. *J. Sea Res.* 124, 17–25. doi: 10.1016/j.seares.2017.04.012

Fritz, L., and Triemer, R. E. (1985). A rapid simple technique utilizing calcofluor white M2R for the visualization of dinoflagellate thecal plates. *J. Phycol.* 21, 662–664. doi: 10.1111/j.0022-3646.1985.00662.x

Fu, G., Baith, K. S., and McClain, C. R. (1998). "SeaDAS: the SeaWiFS data analysis system," in *Proceedings of the 4th Pacific Ocean Remote Sensing Conference*, (Qingdao), 73–79.

García, V. M. T., García, C. A. E., Mata, M. M., Pollery, R. C., Piola, A. R., Signorini, S. R., et al. (2008). Environmental factors controlling the phytoplankton blooms at the Patagonia shelf-break in spring. *Deep Sea Res. Part I* 55, 1150–1166. doi: 10.1016/j.dsr.2008.04.011

Gayoso, A. M., and Fulco, K. (2006). Occurrence patterns of *Alexandrium tamarense* (Lebour) Balech populations in the Golfo Nuevo (Patagonia, Argentina), with observations on ventral pore occurrence in natural and cultured cells. *Harmful Algae* 5, 233–241. doi: 10.1016/j.hal.2004.12.010

Gómez, M. I., Piola, A. R., Kattner, G., and Alder, V. A. (2011). Biomass of autotrophic dinoflagellates under weak vertical stratification and contrasting chlorophyll levels in subantarctic shelf waters. *J. Plankton Res.* 33, 1304–1310. doi: 10.1093/plankt/fbr031

Goyens, C., Jamet, C., and Schroeder, T. (2013). Evaluation of four atmospheric correction algorithms for MODIS-aqua images over contrasted coastal waters. *Remote Sens. Environ.* 131, 63–75. doi: 10.1016/j.rse.2012.12.006

Guinder, V. A., Popovich, C. A., Molinero, J. C., and Perillo, G. M. E. (2010). Long-term changes in the composition, occurrence, timing and magnitude of phytoplankton blooms in the Bahía Blanca estuary. Argentina. *Mar. Biol.* 157, 2703–2716. doi: 10.1007/s00227-010-1530-5

Guinder, V. A., Popovich, C. A., and Perillo, G. M. E. (2009). Particulate suspended matter concentrations in the Bahía Blanca Estuary, Argentina: implication for the development of phytoplankton blooms. *Estuar. Coast. Shelf Sci.* 85, 157–165. doi: 10.1016/j.ecss.2009.05.022

Harðardóttir, S., Pančić, M., Tammilehto, A., Krock, B., Møller, E. F., Nielsen, T. G., et al. (2015). Dangerous relations in the Arctic marine food web: interactions between toxin producing *Pseudo-nitzschia* diatoms and calanus copepodites. *Mar. Drugs* 13, 3809–3835. doi: 10.3390/md13063809

Hasle, G. (1978). "Concentrating phytoplankton. Settling. The inverted microscope method," in *Phytoplankton Manual. Monographs on Oceanographic Methodology*, ed. A. Sournia (Paris: UNESCO), 88–96.

Heileman, S. (2009). "XVI-55 patagonian shelf LME in the UNEP large marine ecosystem report: a perspective on changing conditions in LMES of the world's regional seas," in *UNEP Regional Seas Report and Studies N° 182. United Nations Environment Programme*, eds K. Sherman and G. Hempel (Nairobi: UNDP), 735–746.

Hillebrand, H., Dürselen, C. D., Kirschtel, D., Pollingher, U., and Zohary, T. (1999). Biovolume calculation for pelagic and benthic microalgae. *J. Phycol.* 35, 403–424. doi: 10.1046/j.1529-8817.1999.3520403.x

Hoffmeyer, M. S., Menéndez, M. C., Biancalana, F., Nizovoy, A. M., and Torres, E. R. (2009). Ichthyoplankton spatial pattern in the inner shelf off Bahía Blanca Estuary, SW Atlantic Ocean. *Estuar. Coast. Shelf Sci.* 84, 383–392. doi: 10.1016/j.ecss.2009.07.017

Holm-Hansen, O., Lorenzen, C. J., Holmes, R. W., and Strickland, J. D. H. (1965). Fluorometric determination of chlorophyll. *J. Mar. Sci.* 30, 3–15. doi: 10.1093/icesjms/30.1.3

Hoppenrath, M., and Debres, G. (2009). *Marine Phytoplankton. Selected Microplankton Species From the North Sea Around Helgoland and Sylt*. Stuttgart: Schweitzerbarth Verlag, 264.

Hu, C., Lee, Z., and Franz, B. (2012). Chlorophyll a algorithms for oligotrophic oceans: a novel approach based on three-band reflectance difference. *J. Geophys. Res.* 117:C01011. doi: 10.1029/2011JC007395

Hu, T., Burton, I. W., Cembella, A. D., Curtis, J. M., Quilliam, M. A., Walter, J. A., et al. (2001). Characterization of Spirolides A, C, and 13-Desmethyl C, new marine toxis isolated from toxic plankton and contaminated shellfish. *J. Nat. Prod.* 64, 308–312. doi: 10.1021/np000416q

Jamet, C., Loisel, H., Kuchinke, C. P., Ruddick, K., Zibordi, G., and Feng, H. (2011). Comparison of three SeaWiFS atmospheric correction algorithms for turbid waters using AERONET-OC measurements. *Remote Sens. Environ.* 115, 1955–1965. doi: 10.1016/j.rse.2011.03.018

John, U., Litaker, R. W., Montresor, M., Murray, S., Brosnahan, M. L., and Anderson, D. M. (2014). Formal revision of the *Alexandrium tamarense* species complex (Dinophyceae) taxonmomy: the introduction of five species with emphasis on molecular-based (rDNA) classification. *Protist* 165, 779–804. doi: 10.1016/j.protis.2014.10.001

Keller, M. D., Selvin, R. C., Claus, W., and Guillard, R. R. L. (1987). Media for the culture of oceanic ultraphytoplankton. *J. Phycol.* 23, 633–638. doi: 10.1111/j.1529-8817.1987.tb04217.x

Kopprio, G. A., Streitenberger, M. E., Okuno, K., Baldini, M., Biancalana, F., Fricke, A., et al. (2017). Biogeochemical and hydrological drivers of the dynamics of *Vibrio* species in two Patagonian estuaries. *Sci. Total Environ.* 579, 646–656. doi: 10.1016/j.scitotenv.2016.11.045

Kremp, A., Tahvanainen, P., Litaker, W., Krock, B., Suikkanen, S., Leaw, C. P., et al. (2014). Phylogenetic relationships, morphological variation, and toxin pattern in the *Alexandrium ostenfeldii* (Dinopyhceae) complex: implications for species boundaries and identities. *J. Phycol.* 50, 81–100. doi: 10.1111/jpy.12134

Krock, B., Borel, C. M., Barrera, F., Tillmann, U., Fabro, E., Almandoz, G. O., et al. (2015). Analysis of the hydrographic conditions and cyst beds in the San Jorge Gulf, Argentina, that favor dinoflagellate population development including toxigenic species and their toxins. *J. Mar. Syst.* 148, 86–100. doi: 10.1016/j.jmarsys.2015.01.006

Krock, B., Tillmann, U., John, U., and Cembella, A. D. (2008). LC-MS-MS aboard ship: tandem mass spectrometry in the search for phycotoxins and novel toxigenic plankton from the North Sea. *Anal. Bioanal. Chem.* 392, 797–803. doi: 10.1007/s00216-008-2221-7

Kumar, S., Stecher, G., and Tamura, K. (2016). MEGA7: molecular evolutionary genetics analysis version 7.0 for bigger datasets. *Mol. Biol. Evol.* 33, 1870–1874. doi: 10.1093/molbev/msw054

Le Quéré, C., Harrison, S. P., Prentice, I. C., Buitenhuis, E. T., Aumont, O., Bopp, L., et al. (2005). Ecosystem dynamics based on plankton functional types for global ocean biogeochemistry models. *Glob. Change Biol.* 11, 2016–2040.

Lilly, E. L., Halanich, K. M., and Anderson, D. M. (2007). Species boundaries and global biogeography of the *Alexandrium tamarense* complex (Dinophyceae). *J. Phycol.* 43, 1329–1338. doi: 10.1111/j.1529-8817.2007.00420.x

Litchman, E., and Klausmeier, C. A. (2008). Trait-based community ecology of phytoplankton. *Annu. Rev. Ecol. Evol. S.* 39, 615–639. doi: 10.1146/annurev.ecolsys.39.110707.173549

Liu, K.-K., Atkinson, L., Quinones, R. A., and Talaue-McManus, L. (2010). "Biogeochemistry of continental margins in a global context," in *Carbon and Nutrient Fluxes in Continental Margins. A Global Synthesis*, eds K.-K. Liu, L. Atkinson, R. A. Quinones, and L. Talaue-McManus (Berlin: Springer), 3–24. doi: 10.1007/978-3-540-92735-8_1

López Abbate, M. C., Molinero, J. C., Guinder, V. A., Dutto, M. S., Barría de Cao, M. S., Ruiz Etcheverry, L. A., et al. (2015). Microplankton dynamics under heavy anthropogenic pressure. The case of the Bahía Blanca Estuary, southwestern Atlantic Ocean. *Mar. Pollut. Bull.* 95, 305–314. doi: 10.1016/j.marpolbul.2015.03.026

López Abbate, M. C., Molinero, J. C., Guinder, V. A., Perillo, G. M., Freije, R. H., Sommer, U., et al. (2017). Time-varying environmental control of phytoplankton in a changing estuarine system. *Sci. Total Environ.* 609, 1390–1400. doi: 10.1016/j.scitotenv.2017.08.002

López Cazorla, A., Molina, J. M., and Ruarte, C. (2014). The artisanal fishery of *Cynoscion guatucupa* in Argentina: exploring the possible causes of the collapse in Bahía Blanca estuary. *J. Sea Res.* 88, 29–35. doi: 10.1016/j.seares.2013.12.016

Lucas, A. J., Guerrero, R. A., Mianzán, H. W., Acha, M. E., and Lasta, C. A. (2005). Coastal oceanographic regimes of the Northern Argentine continental Shelf (34-43°S). *Estuar. Coast. Shelf Sci.* 65, 405–420. doi: 10.1016/j.ecss.2005.06.015

Lutz, V. A., Segura, V., Dogliotti, A. I., Gagliardini, D. A., Bianchi, A., and Balestrini, C. E. (2010). Primary production in the Argentine Sea during spring estimated by field and satellite models. *J. Plankton Res.* 32, 181–195. doi: 10.1093/plankt/fbp117

Marrari, M., Delia Viñas, M., Martos, P., and Hernández, D. (2004). Spatial patterns of mesozooplankton distribution in the Southwestern Atlantic Ocean (34–41°S) during austral spring: relationship with the hydrographic conditions. *ICES J. Mar. Sci.* 61, 667–679. doi: 10.1016/j.icesjms.2004.03.025

Marrari, M., Piola, A. R., and Valla, D. (2017). Variability and 20-year trends in satellite-derived surface chlorophyll concentrations in large marine ecosystems around South and Western Central America. *Front. Mar. Sci.* 4:372. doi: 10.3389/fmars.2017.00372

Marrari, M., Signorini, S., McClain, C. R., Pájaro, M., Martos, P., Viñas, M. D., et al. (2013). Reproductive success of the Argentine anchovy, *Engraulis anchoita*, in relation to environmental variability at a mid-shelf front (Southwestern Atlantic Ocean). *Fish. Oceanogr.* 22, 247–261. doi: 10.1111/fog.12019

Matano, R. P., Palma, E. D., and Piola, A. R. (2010). The influence of the Brazil and Malvinas currents on the southwestern Atlantic shelf. *Ocean Sci.* 6, 983–995. doi: 10.5194/os-6-983-2010

Menden-Deuer, S., and Lessard, E. J. (2000). Carbon to volume relationships for dinoflagellates, diatoms, and of the protist plankton. *Limnol. Oceanogr.* 45, 569–579. doi: 10.4319/lo.2000.45.3.0569

Montoya, N. G., Akselman, R., Franco, J., and Carreto, J. I. (1996). "Paralytic shellfish toxins and mackerel (Scomber Japonicus) mortality in the Argentine Sea," in *Harmful and Toxic Algal Blooms Intergovernmental Oceanographic Commission (IOC) of UNESCO*, eds T. Yasumoto, Y. Oshima, and Y. Fukuyo (Paris: UNESCO), 417–420.

Montoya, N. G., Fulco, V. K., Carignan, M. O., and Carreto, J. I. (2010). Toxin variability in cultured and natural populations of *Alexandrium tamarense* from southern South America - evidences of diversity and environmental regulation. *Toxicon* 56, 1408–1418. doi: 10.1016/j.toxicon.2010.08.006

Negri, R. M., Montoya, N., Carreto, J. I., Akselman, R., and Inza, D. (2004). "*Pseudo-nitzschia* australis, *Mytilus edulis*, *Engraulis anchoita* and domoic acid in the Argentine Sea," in *Florida Fish and Wildlife Conservation Commission, Florida Institute of Oceanography, and Intergovernmental Oceanographic Commission of UNESCO*, (St. Petersburg), 139–141.

Negri, R. M., Silva, R. I., Segura, V., and Cucchi Colleoni, D. (2013). Estructura de la comunidad del fitoplancton en el área de "El Rincón", Mar Argentino (Febrero 2011). *Rev. Invest. Desarr. Pesq.* 23, 7–22.

Olguín, H. F., Brandini, F., and Boltovskoy, D. (2015). Latitudinal patterns and interannual variations of spring phytoplankton in relation to hydrographic conditions of the southwestern Atlantic Ocean (34-62 S). *Helgoland Mar. Res.* 69:177. doi: 10.1007/s10152-015-0427-6

Orr, R. J. S., Stuken, A., Rundberget, T., Eikrem, W., and Jakobsen, K. S. (2011). Improved phylogenetic resolution of toxic and non-toxic *Alexandrium* strains using a concatenated rDNA approach. *Hamful Algae* 10, 676–688. doi: 10.1016/j.hal.2011.05.003

Palma, E. D., and Matano, R. P. (2012). A numerical study of the Magellan plume. *J. Geophys. Res.* 117, 1–16. doi: 10.1029/2011JC007750

Palma, E. D., Matano, R. P., and Piola, A. R. (2008). Numerical study of the Southwestern Atlantic Shelf circulation: stratified ocean response to local and offshore forcing. *J. Geophys. Res.* 113, 1–24. doi: 10.1029/2007JC004720

Paniagua, G. F., Saraceno, M., Piola, A. R., Guerrero, R., Provost, C., Ferrari, R., et al. (2018). Malvinas current at 408S–418S: first assessment of temperature and salinity temporal variability. *J. Geophys. Res. Oceans* 123, 5323–5340. doi: 10.1029/2017JC013666

Park, M. G., Kim, S., Kim, H. S., Myung, G., Kang, Y. G., and Yih, W. (2006). First successful culture of the marine dinoflagellate *Dinophysis acuminata*. *Aquat. Microb. Ecol.* 45, 101–106. doi: 10.3354/ame045101

Penna, A., Fraga, S., Masó, M., Giacobbe, M. G., Bravo, I., Garcés, E., et al. (2008). Phylogenetic relationships among the Mediterranean *Alexandrium* (Dinophyceae) species based on sequences of 5.8 S gene and Internal Transcript Spacers of the rRNA operon. *Eur. J. Phycol.* 43, 163–178. doi: 10.1080/09670260701783730

Reguera, B., Riobó, P., Rodríguez, F., Díaz, P. A., Pizarro, G., Paz, B., et al. (2014). Dinophysis toxins: causative organisms, distribution and fate in shellfish. *Mar. Drugs* 12, 394–461. doi: 10.3390/md12010394

Roach, J. S., LeBlanc, P., Lewis, N. I., Munday, R., Quilliam, M. A., and MacKinnon, S. L. (2009). Characterization of a dispiroketal spirolide subclass from *Alexandrium ostenfeldii*. *J. Nat. Prod.* 72, 1237–1240. doi: 10.1021/np800795q

Romero, S. I., Piola, A. R., Charo, M., and Garcia, C. A. E. (2006). Chlorophyll-a variability off Patagonia based on SeaWiFS data. *J. Geophys. Res. Oceans* 111, C05021. doi: 10.1029/2005JC003244

Salgado, P., Riobó, P., Rodríguez, F., Franco, J. M., and Bravo, I. (2015). Differences in the toxin profiles of *Alexandrium ostenfeldii* (Dinophyceae) strains isolated from different geographic origins: evidence of paralytic toxin, spirolide, and gymnodimine. *Toxicon* 103, 85–98. doi: 10.1016/j.toxicon.2015.06.015

Sar, E. A., Sunsen, I., Goya, A. B., Lavigne, A. S., Tapias, E., García, C., et al. (2012). First report of diarrheic shellfish toxins in mollusks from buenos aires province (Argentina) associated with *Dinophysis* spp.: evidence of okadaic acid, dinophysis toxin-1 and their acyl derivatives. *Bol. Soc. Argent. Bot.* 47, 5–14.

Segura, V., Lutz, V. A., Dogliotti, A., Silva, R. I., Negri, R. M., Akselman, R., et al. (2013). Phytoplankton types and primary production in the Argentine Sea. *Mar. Ecol. Prog. Ser.* 491, 15–31. doi: 10.3354/meps10461

Silva, R. I., Negri, R., and Lutz, V. (2009). Summer succession of ultraphytoplankton at the EPEA coastal station (northern Argentina). *J. Plankton Res.* 31, 447–458. doi: 10.1093/plankt/fbn128

Sleno, L., and Volmer, D. A. (2005). Toxin screening in phytoplankton: detection and quantitation using MALDI triple quadruploe mass spectrometry. *Anal. Chem.* 77, 1509–1517. doi: 10.1021/ac0486600

Tillmann, U. (2018a). "Amphidomataceae," in *Harmful Algae Blooms, a Compendium Desk Reference*, eds S. E. Shumway, J. A. Burkholder, and S. L. Morton (Hoboken, NJ: Wiley-Blackwell). doi: 10.1002/9781118994672.ch16b

Tillmann, U. (2018b). Electron microscopy of a 1991 spring plankton sample from the Argentinean Shelf reveals the presence of four new species of the Amphidomataceae (Dinophyceae). *J. Phycol. Res.* 66, 269–290. doi: 10.1111/pre.12225

Tillmann, U., and Akselman, R. (2016). Revisiting the 1991 algal bloom in shelf waters off Argentina: *Azadinium luciferelloides* sp nov. (Amphidomataceae, Dinophyceae) as the causative species in a diverse community of other amphidomataceans. *Phycol. Res.* 64, 160–175. doi: 10.1111/pre.12133

Tillmann, U., Borel, C. M., Barrera, F., Lara, R., Krock, B., Almandoz, G., et al. (2016). *Azadinium poporum* from the Argentine Continental Shelf, Southwestern Atlantic, produces azaspiracid-2 and azaspiracid-2 phosphate. *Harmful Algae* 51, 40–55. doi: 10.1016/j.hal.2015.11.001

Tillmann, U., Gottschling, M., Guinder, V., and Krock, B. (2018). *Amphidoma parvula* (Amphidomataceae), a new planktonic dinophyte from the Argentine Sea. *Eur. J. Phycol.* 53, 14–28. doi: 10.1080/09670262.2017.1346205

Tomas, C. R. (ed.) (1997). *Identifying Marine Phytoplankton*. Amsterdam: Elsevier, 858.

Trainer, V. L., Bates, S. S., Lundholm, N., Thessen, A. E., Cochlan, W. P., Adams, N. G., et al. (2012). *Pseudo-nitzschia* physiological ecology, phylogeny, toxicity, monitoring and impacts on ecosystem health. *Harmful Algae* 14, 271–300. doi: 10.1016/j.hal.2011.10.025

Van de Waal, D. B., Tillmann, U., Martens, H., Krock, B., van Scheppingen, Y., and John, U. (2015). Characterization of multiple isolates from an *Alexandrium ostenfeldii* bloom in the Netherlands. *Harmful Algae* 49, 94–104. doi: 10.1016/j.hal.2015.08.002

Winder, M., Carstensen, J., Galloway, A. W. E., Jakobsen, H. H., and Cloern, J. E. (2017). The land-sea interface: a source of high-quality phytoplankton to support secondary production. *Limnol. Oceanogr.* 62, S258–S271. doi: 10.1002/lno.10650

Conflict of Interest Statement: The authors declare that the research was conducted in the absence of any commercial or financial relationships that could be construed as a potential conflict of interest.